Poly(vinyl pyrrolidone) Derivatives as PEG Alternatives for Stealth, Non-toxic and Less Immunogenic siRNA-Containing Lipoplex Delivery

Manon Berger[1], François Toussaint[2*], Sanaa Ben Djemaa[3*], Julie Laloy[4], Hélène Pendeville[5], Brigitte Evrard[1], Christine Jerôme[2], Anna Lechanteur[1], Denis Mottet[3**], Antoine Debuigne[2**], Geraldine Piel[1**]*

[1] Laboratory of Pharmaceutical Technology and Biopharmacy, CIRM, University of Liege, Belgium

[2] Center for Education and Research on Macromolecules (CERM), CESAM Research Unit, University of Liege, Belgium

[3] Gene Expression and Cancer Laboratory (GEC), GIGA-Molecular Biology of Diseases, University of Liege, Belgium

[4] NNC Laboratory (NARILIS), Department of Pharmacy, University of Namur, Belgium

[5] Platform Zebrafish Facility and Transgenics, GIGA, University of Liège, Belgium

* Co-first authors

** Co-last authors and corresponding authors (Geraldine.Piel@uliege.be, adebuigne@uliege.be, dmottet@uliege.be)

Keywords: Lipoplexes, Protein Corona, Immune reaction, Stealth Properties, PEG derivatives, Poly(vinyl pyrrolidone)

Abstract

The recent approval of Onpattro® and COVID-19 vaccines has highlighted the value of lipid nanoparticles (LNPs) for the delivery of genetic material. If it is known that PEGylation is crucial to confer stealth properties to LNPs, it is also known that PEGylation is responsible for the decrease of the cellular uptake and endosomal escape and for the production of anti-PEG antibodies inducing accelerated blood clearance (ABC) and hypersensitivity reactions. Today, the development of PEG alternatives is crucial. Poly(N-vinyl pyrrolidone) (PNVP) has shown promising results for liposome decoration but has never been tested for the delivery of nucleic acids. Our aim is to develop a series of amphiphilic PNVP compounds to replace lipids-PEG for the post-insertion of lipoplexes dedicated to siRNA delivery. PNVP compounds with different degrees of polymerization and hydrophobic segments, such as octadecyl and dioctadecyl and 1,2-distearoyl-sn-glycero-3-phosphoethanolamine (DSPE), were generated. Based on the physicochemical properties and the efficiency to reduce protein corona formation, we showed that the DSPE segment is essential for the integration into the lipoplexes. Lipoplexes post-grafted with 15% DSPE-$PNVP_{30}$ resulted in gene silencing efficiency close to that of lipoplexes grafted with 15% DSPE-PEG. Finally, an *in vivo* study in mice confirmed the stealth properties of DSPE-$PNVP_{30}$ lipoplexes as well as a lower immune response ABC effect compared to DSPE-PEG lipoplexes. Furthermore, we showed a lower immune response after the second injection with DSPE-$PNVP_{30}$ lipoplexes compared to DSPE-PEG lipoplexes. All these observations suggest that DSPE-$PNVP_{30}$ appears to be a promising alternative to PEG, with no toxicity, good stealth properties and lower immunological response.

1 Introduction

The recent development of COVID-19 vaccines has shown that lipid nanoparticles (LNPs) and gene delivery have the potential to revolutionize vaccine development. Indeed, two of the most widely used COVID vaccines, Comirnaty® et Spikevax® are composed of mRNA complexed in a novel ionizable lipid nanoparticle [1,2]. In addition to vaccination, the use of lipid nanovectors such as LNPs carrying mRNA or siRNA could also help to treat difficult-to-treat diseases [3]. In this context, the 2018 FDA approval of Onpattro® (Patisiran) highlighted the growing interest of pharmaceutical research in gene delivery. Onpattro®, the first FDA-approved RNAi drug, is indicated for the treatment of hereditary ATTR amyloidosis [4]. Interestingly, Onpattro® and the LNP-COVID vaccines have a similar composition: an ionizable lipid, two auxiliary lipids and a amphiphilic polyethylene glycol lipid (lipid-PEG) [2,5,6].

The use of lipid-PEG in LNP formulations is crucial to increase the blood circulation time and tumor accumulation, as PEG confers stealth properties by preventing nanoparticles recognition and uptake by the reticuloendothelial system (RES) [7–9]. PEG is thus commonly used to prevent protein corona formation around the nanoparticles. Indeed, without PEG grafting, particles are rapidly covered by blood proteins following intravenous injection, leading to the formation of a protein corona. This corona is responsible for changes in physicochemical properties (such as size increase), pharmacokinetics, biodistribution, targeting capacity and cellular uptake, complement activation and consequently liposomes rapid clearance [10]. The adsorption of blood proteins is a complex phenomenon that depends on many factors such as the type, size, shape and charge of the nanoparticles but also the biological environment, pH, temperature, dynamic shear stress…[10,11].

While PEG is crucial to enhance blood circulation time, polymer grafting is also known to reduce interactions between lipid particles and cell membranes which decreases cellular uptake and

endosomal escape, thus ultimately prevents siRNA delivery and gene silencing. This is the so-called *PEG dilemma*.

Moreover, immunogenicity problems can occur with repeated administration of PEGylated liposomes as anti-PEG IgM antibodies are produced after the first administration. The consequence of this antibody production can be the "accelerated blood clearance (ABC)", a phenomenon which is responsible for the rapid clearance of PEGylated liposomes after subsequent administrations. Finally, hypersensitivity reactions (HSRs) can also occur and induce potentially severe allergic reactions [9,12,13]. In 2021, De Vrieze *et al.* reported severe allergic reactions to the COVID-19 vaccines (11.1 cases per million doses of vaccine) which is much higher than other vaccines (approximately one case per million doses of vaccine) [14]. These immunogenic issues must therefore be seriously considered, especially as an increasing number of healthy patients have pre-existing anti-PEG antibodies related to frequent cosmetic use for instance [13,15].

As many treatment strategies require multiple doses, the development of PEG alternatives that do not promote an immune response but maintain a long blood circulation time is crucial. Polymers intended to provide protein repellence around liposome or LNP must meet certain general requirements. They should be highly water soluble, have good biocompatibility and be easy to synthesize. Among polymers that have been tested as an alternative to PEG [15–18], namely poly(glycerols), poly[N-(2-hydroxypropyl) methacrylamide] (HPMA), poly(2-methyl-2-oxazoline) (PMOX), poly(N-acryloyl morpholine) (PAcM), poly(N,N-dimethylacrylamide) (PDMA) and poly(N-vinyl pyrrolidone) (PNVP), the latter is particularly attractive due to its hydrophilicity, biocompatibility and wide use for biomedical applications [19–24]. A few pioneer studies have notably lifted the veil on the potential of PNVP for liposomes decoration [17,25–27]. Negatively charged liposomes (PC/Chol/CL phosphatidylcholine/cholesterol/cardiolipin) were

formulated in the presence of ill-defined stearyl-PNVP compounds which inhibited their interactions with polycations and increased their stability in mouse serum [25]. Such PNVP-modified liposomes were loaded with nystatin and amphotericin B leading to higher antifungal activity than non-immobilized antibiotics [26]. Unloaded PNVP-decorated liposomes composed of hydrogenated soybean phosphatidylcholine/cholesterol/1,1-dioctadecyl-3,3,3',3'-tetramethylindocarbocyanine perchlorate (HSPC/Chol/DiD) also showed extended circulation times without eliciting an accelerated clearance upon repeated administration [17].

However, to our knowledge, PNVP has never been reported as an alternative to PEG for the decoration of lipoplexes developed for the delivery of siRNAs. In this study, we aim to design a series of amphiphilic PNVP compounds to replace lipids-PEG traditionally used for post-insertion of lipoplexes dedicated to siRNA delivery (**Figure 1**). A library of well-defined PNVP derivatives with different degrees of polymerization (DP) and various hydrophobic segments was generated. Single and dual aliphatic chains, such as octadecyl (OD) and dioctadecyl (DiOD), as well as 1,2-distearoyl-sn-glycero-3-phosphoethanolamine (DSPE) were considered as hydrophobic groups whereas PNVPs segments with low dispersity and specific molar masses were synthesized by reversible addition fragmentation chain transfer (RAFT) polymerization.

The ability of the new PNVP derivatives to replace DSPE-PEG for post-insertion into siRNA-lipoplexes (1,2-dioleoyl-3-trimethylammonium-propane/Cholesterol/1,2-dioleoyl-sn-glycero-3-phosphoethanolamine) (DOTAP/Chol/DOPE 1/0.75/0.5, 100 nM siRNA, N/P 2.5) was investigated. Following polymers synthesis and characterizations, several formulations of PNVP grafted lipoplexes have been produced and analyzed in terms of physicochemical properties, safety, cellular uptake, immunogenicity and biodistribution in mice.

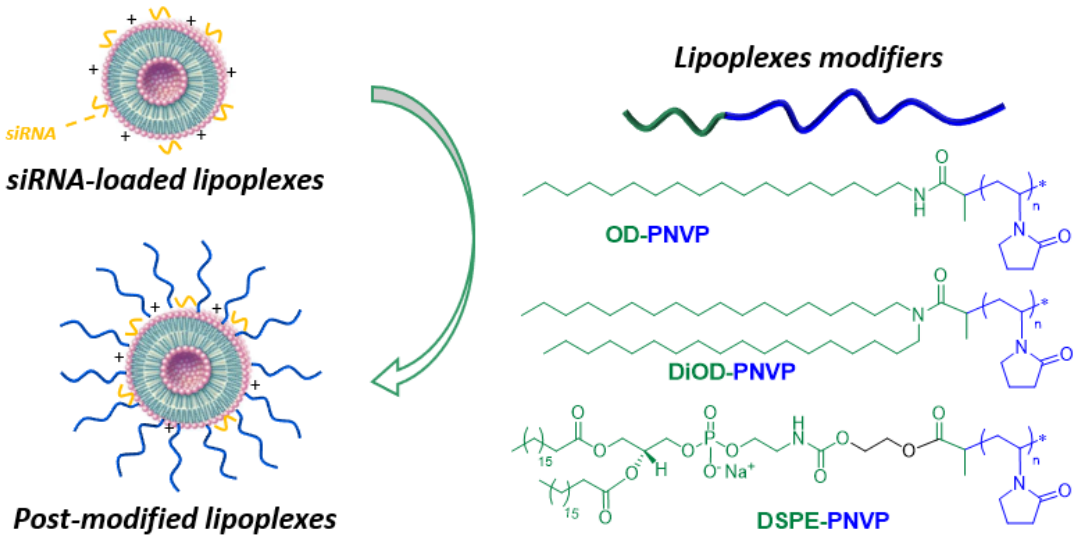

Figure 1: Post-modification of siRNA-loaded lipoplexes with amphiphilic PNVP derivatives.

2 Materials and Methods

2.1 Synthesis of the PNVP Derivatives

The multi-step synthesis of the PNVP derivatives, namely Ethyl (Et)-PNVP, OD-PNVP, DiOD-PNVP and DSPE-PNVP, is described in detail in the supporting information section (**Schemes S1-S4**). Characteristics of the polymers are provided in Tables S1-S4. Nuclear magnetic resonance (NMR) and size exclusion chromatography (SEC) analyses of the polymers and of their intermediates are provided in **Figures S1-S4.**

2.2 Preparation of Liposome and Lipoplex Formulations

Cationic liposomes were prepared by the thin lipid film hydration method as previously described [28–32]. Briefly, a dried lipid film was prepared with DOTAP, cholesterol and DOPE (1/0.75/0.5 molar ratio) at a final lipid concentration of 5.5 mM. The lipid film was hydrated with RNAse-free water (ThermoFisher Scientific, Walthman, MA, USA), vortexed and directly extruded (Lipex™

Extruder, Tansferra Nanosciences Inc., Burnaby, Canada) through polycarbonate membranes (5 times on 400 nm and 10 times on 200 nm). DOTAP and DOPE were purchased from Avanti Polar Lipids, Inc. (Alabaster, AL, USA). Cholesterol was purchased from Sigma Aldrich (Belgium).

The cationic liposomes were then complexed to anionic siRNA by spontaneous charge interaction to form lipoplexes. Liposomes and siRNA were mixed during 30 min at a N/P ratio of 2.5. siRNA targeted EGFP (siGFP), an irrelevant siRNA directed against non-human luciferase gene (siGL3) and fluorescent negative control siRNA (siGL3 Cy 5 and Cy 5.5) were provided by Eurogentec® (Eurogentec SA, Liège, Belgium). The corresponding sequences are the following: siGFP: sense strand: 5'-GCAAGCUGACCCUGAAGUUC55-3', antisense strand: 5'-GAACUUCAGGGUCAGCUUGC55-3'; siGL3: sense strand: 5'-CUUACGCUGAGUACUUCGAUU55-3', antisense strand: 5'-AAUCGAAGUACUCAGCGUAAG55-3'; siGL3 Cy5 and Cy5.5 are siGL3 chemically conjugated with Cy5® or Cy5.5® dyes at the 5'-end of the sense strand.

Lipoplexes were then post-grafted under a stirring process by the addition of the polymers at different molar ratios (5, 10, 15, 30 or 40 mol% compared to the total of lipid). Briefly, polymers in RNAse-free water (1 mM) were added to preformed lipoplexes. The resulting mixture was vortexed for 15 seconds and maintained 1 h at 37°C [30]. 1,2-distearoyl-sn-glycero-3-phosphoethanolamine-N-[methoxy(polyethylene glycol)-2000] (DSPE-PEG) was purchased from Avanti Polar Lipids, Inc. (Alabaster, AL, USA) and the amphiphilic PNVP derivatives were synthetized as described in the section 2.1.

2.3 Physicochemical Characterizations

2.3.1 Size, PdI and Surface Charge

The size (Z-average size) (nm) and the polydispersity index (PdI) of lipoplexes were determined by Dynamic Light Scattering (DLS) using the Malvern Zetasizer® (Nano ZS, Malvern Instrument, UK) in RNAse-free water with a fixed angle of 90°. The zeta potential (Zp) (mV) was determined with the same instrument. All of the experiments were done in triplicate (n=3) at 25°C.

2.3.2 Complexation Efficiency

The uncomplexed siRNA was quantified using a Quant-it™ RiboGreen® RNA assay (Invitrogen™ (ThermoFisher Scientific, Walthman, MA, USA)) according to the manufacturer's instructions. Samples of lipoplexes (100 nM siRNA) and siRNA calibration curves were prepared as previously described [28]. 100 µl of RiboGreen® reagent was added to each well and fluorescence was measured with the FlexStation 3 Multi-Mode Microplate Reader (Molecular Devices, CA, USA). Wavelengths of excitation and emission were 485 and 530 nm, respectively. The detected fluorescence was calculated related to the concentration of free siRNA according to the blank and the calibration curves. The level of complexed siRNA was then determined.

2.3.3 Membrane Interaction

QCM-D analyses of the polymer/membrane interactions were adapted from previous works [33,34]. Gold coated sensors (Q-Sense AT-cut quartz crystals, fundamental frequency of 5 MHz) were cleaned and functionalized by mercaptopropionic acid as reported elsewhere [33,34]. DOTAP/Chol/DOPE (1/0.75/0.5 molar ratio) liposomes were prepared as described above except that the lipid film was rehydrated with high salt PBS buffer (20 mM PBS and 100 mM NaCl) instead of RNAse-free water (final liposome concentration of 5.5 mM). Deposition of the

DOTAP/Chol/DOPE membrane onto the sensor was achieved following the membrane deposition method reported by Martin *et al.* [33,34]. Briefly, the sensor was exposed successively to high salt PBS buffer (20 mM PBS and 100 mM NaCl), liposome solution (0.1 mM in high salt PBS), high salt PBS buffer to remove excess of liposomes, low salt PBS buffer (20 mM PBS and 30 mM NaCl) to break the liposomes membranes by osmotic pressure, high salt PBS buffer to remove weakly bound lipids. Proper deposition of the DOTAP/Chol/DOPE membrane was confirmed by a Δf of about 14 Hz. The accordingly modified sensor surface was then exposed to solutions of the different PNVP derivatives (30 µM in high salt PBS buffer).

2.4 Protein Corona Formation

Protein corona formation was evaluated by Nanoparticle Tracking Analysis (NTA). NTA measurements were performed using NanoSight NS300 (Malvern Instruments Ltd., UK) equipped with a 642 nm red laser module. The protocol was inspired by Karim *et al.* [35]. Lipoplexes were mixed with heat-inactivated (HI) fetal bovine serum (FBS) (Gibco (Invitrogen™, ThermoFisher Scientific, Walthman, MA, USA)) at a 2:1 ratio (v/v) and incubated for 2 hours at 37°C under stirring process. The FBS concentration was chosen to mimic physiological conditions. The formation of the protein corona around the lipoplexes was assessed by measuring the evolution of the particle mean size from time 0 to 2 hours after the addition of FBS. Samples were measured in triplicate (n=3) at 25°C with the red laser and syringe pump speed of 40 (arbitrary unit).

2.5 Toxicity Evaluation

2.5.1 Cell Culture

Human lung adenocarcinoma cells A549 were obtained from the American Type Culture Collection (ATCC, University Blvd, Manassas, VA, USA). A549 cells and A549 cells stably

expressing GFP (A549/GFP) were maintained in Dulbecco's modified Eagle medium (DMEM) (Biowest, VWR, Leuven, Belgium) supplemented with 10% FBS and 1% of PenStrep® (Gibco (Invitrogen™, ThermoFisher Scientific, Walthman, MA, USA)) at 37°C in 5% CO_2-humidified atmosphere.

2.5.2 Cell Viability Assay

A549 cells were seeded in 96-well plates (5 x 10^3 cells/well). After 24 h, cells were incubated for 4 h with different concentrations of polymers (different molar ratios from 5 to 150 mol% compared to the total of lipid used in the lipoplex formulations) or lipoplexes (naked and grafted lipoplexes) in Opti-MEM™ (Gibco (Invitrogen™, ThermoFisher Scientific, Walthman, MA, USA)) prepared at a concentration of 100 nM of siGL3. Then, the formulations were replaced by fresh culture medium containing 10% (v/v) MTT (3-(4,5-Dimethylthiazol-2-yere)-2,5-Diphenyltetrazolium Bromide) reagent (Invitrogen™ by ThermoFisher Scientific, Bleiswijk, Netherlands), for 3 h at 37°C. Non-treated cells were used as the negative control and cells treated with hydrogen peroxide solution (H_2O_2, Sigma-Aldrich Chimie GmbH) at 20 mM were used as positive control. The absorbance was measured at 450 nm using MikroWin 2010 software (Labsis Laborsysteme GmbH, Neunkirchen-Seelscheid, Germany) on a TriStar^{2}S LB 942 multimode reader (Berthold Technologies, Vilvoorde, Belgium). The number of viable cells is directly proportional to the absorbance value.

2.5.3 Apoptosis Assay

A549 cells were seeded in 12-well plates (1.8 x 10^5 cells/well). After 24 h, cells were incubated in Opti-MEM™ with naked lipoplexes or grafted lipoplexes prepared with siGL3 at 100 nM. After 24 h, cells were washed with PBS, harvested with Trypsin-EDTA® and collected. The staining of cells was performed using BD Pharmingen™ FITC Annexin V Apoptosis Detection Kit (BD

Biosciences, Erembodegem, Belgium) according to manufacturer's instructions. Cells were analyzed using CytExpert software in CytoFLEX flow cytometer (Beckman Coulter, Inc., US).

2.5.4 *In vivo* Acute Toxicity in Zebrafish Model

Adult zebrafish (*Danio rerio*) were maintained while fulfilling the criteria of the Ethical Committee for the Use of Laboratory Animals at the University of Liege (Protocol #21-2313). Fertilized eggs were collected, washed with E3 medium, and placed in petri dishes. Fertilized eggs were incubated at 28°C and maintained on a 14 h day/10 h night period throughout the experiment. Embryos were collected at 24 hours post-fertilization (hpf), their chorions were removed and the toxicity of lipoplexes was evaluated. 10 embryos were used per condition in 12-well plates. Embryos were treated once a day for two days and were observed daily for up to 72 hpf. Each well contained 1.5 ml of E3 medium containing 100 µl of naked lipoplexes or grafted lipoplexes (15% polymer, 1 and 10g siGL3/kg). E3 medium stock solution is composed of 34.8 g NaCl, 1.6 g KCl, 5.8 g $CaCl_2 \cdot 2H_2O$, 9.78 g $MgCl_2 \cdot 6H_2O$ for a final volume of 2 L of H_2O. The pH is adjusted to 7.2 with NaOH. The E3 stock solution is diluted 60x before use and 100 µL of 1% methylene blue are added. Treatment dose was replaced once daily for two days, and embryos were observed each day until 72 hpf.

2.5.5 Hemocompatibility Assay

Hemolysis was tested based on Drabkin method. Briefly, washed red blood cells from three healthy donors were incubated with lipoplexes for 1 h at 37°C or room temperature (RT) in the presence of 5% CO_2. After centrifugation, the supernatant is collected, and hemoglobin concentration is determined by spectrometric detection of cyanmethemoglobin at 540 nm and expressed in percentage compared to Triton X-100 (inducing 100% of hemolysis). Platelet aggregation was tested using a protocol previously described [36] and using a final concentration of lipoplexes of

200 nM siRNA. Polymers were tested at 15% molar ratio of total lipids. The study protocol was in accordance with the Declaration of Helsinki and was approved by the Medical Ethical Committee of the Centre Hospitalier Universitaire (CHU), UCL Namur (Yvoir, Belgium).

2.6 Cell Uptake and siRNA Efficiency

2.6.1 Cellular Internalization

A549 cells were seeded in 24-well plates (1 x 10^5 cells/well). After 24 h, lipoplexes prepared with 100 nM of siRNA conjugated to Cy5 (siGL3 Cy5) were added to cells for 4 h. Non-treated cells were used as negative control. After treatment, cells were washed with PBS, harvested with Trypsin-EDTA® and re-suspended in PBS. 1x10^4 cells were analyzed by BD FACS Canto™ II flow cytometer (BD Biosciences, Franklin Lakes, USA) to measure the intracellular fluorescence of Cy5.

2.6.2 Gene Silencing Efficiency

A549/GFP cells were seeded in 6-well plates (1.8 x 10^5 cells/well). After 24 h, cell culture medium was replaced by 1 mL of Opti-MEM™ containing lipoplexes and grafted lipoplexes prepared with 100 nM of siRNA EGFP (siGFP). Lipofectamine® RNAiMAX (ThermoFisher Scientific, Walthman, MA, USA) associated with EGFP siRNA was used as the positive control. Cells were incubated for 4 h at 37°C and then, the formulations were replaced by fresh culture medium. After 72 h, cells were washed with PBS pH 7.4, harvested with Trypsin-EDTA® and re-suspended in 300 µL of PBS. 1 x 10^4 cells were analyzed by CytoFLEX flow cytometer to measure the GFP fluorescence intensity of A549 cells.

2.7 *In vivo* Evaluation

2.7.1 Animals

Female BALB/c mice aged 8 weeks (20–25 g) were purchased from Janvier Labs (Saint-Berthevin, France). All animal experiments were evaluated and approved by the Animal and Ethics Review Committee of the University of Liege (Protocol #21-2397). During the study, animals were housed in a controlled climate and photoperiod (12 h light-dark cycles) and had free access to water and food. Three groups with 8 mice/group were divided as following: (i) a control group injected with PBS, (ii) a group injected with DSPE-PEG lipoplexes, and (iii) a group injected with DSPE-$PNVP_{30}$ lipoplexes prepared at a concentration of 1 mg/kg of siGL3 Cy5.5.

2.7.2 *In vivo* Biodistribution and ABC Effect in Mice

The biodistribution and ABC effect were investigated after intravenous injection of 100 µl of grafted lipoplexes (15% DSPE-PEG and DSPE-$PNVP_{30}$ polymer) containing 1 mg/kg of control siGL3 Cy5.5 at N/P 2.5 and isotonized with mannitol, once a week for two weeks. *In vivo* fluorescence imagining was performed on live animals 5 h and 24 h after each injection using Living Image® software in IVIS Spectrum *In Vivo* Imaging System (PerkinElmer).

One week after the second injection, mice were sacrificed, and the main organs (liver, kidney, heart, spleen, and lung) were removed to perform *ex-vivo* fluorescence imaging.

2.7.3 Detection of IgG and IgM anti-PEG or anti-PNVP Antibodies and Pro-Inflammatory Cytokines

Blood was collected from mice tails on day 7 after the first injection and by cardiac puncture on day 14. To obtain serum, the blood was placed at RT for 30 min and then centrifuged at 1000 g at 4°C for 15 min.

The serum collected from mice injected with PBS was used as a negative control. A direct ELISA procedure was employed to detect PEG- or PNVP-specific IgM and IgG antibodies in the serum. Briefly, 2 µg of DSPE-PEG or DSPE-$PNVP_{30}$ in ethanol was added to 96-well plates. Coated plates were allowed to completely air dry. The plates were then washed with PBS and then blocked for 1 h with PBS containing 2% BSA. Diluted serum samples (1:1000) were then added in wells, incubated for 1 h and washed five times with PBS. Horseradish peroxidase (HRP)-conjugated antibody diluted 1/1000 in PBS (Goat anti-mouse IgM-HRP (Invitrogen™, Camarillo, USA) or Goat anti-mouse IgG-HRP (Cell Signaling, Leiden, The Netherlands)) were added in wells. After 45 min, wells were washed five times with PBS. The coloration was initiated by adding TMB (Invitrogen™). After 30 min, the reaction was stopped by adding sulfuric acid 2 M. The absorbance was measured at 450 nm using MikroWin 2010 software (Labsis Laborsysteme GmbH, Neunkirchen-Seelscheid, Germany) on a TriStar²S LB 942 multimode reader (Berthold Technologies, Bad Wildbad, Germany). All incubations were performed at RT using a plate shaker (300 rpm).

IL-1β and TNF-α pro-inflammatory cytokines were analyzed in postmortem serum using commercial ELISA kits (Mouse IL-1 beta ELISA kit and Mouse TNF-alpha ELISA kit; Invitrogen™, Vienna, Austria). The dosage was performed according to manufacturer's procedures.

2.8 Statistics

Values were expressed as means ± standard deviations (SD) for at least n=3. GraphPad Prism 7 was used for statistical analysis. Data were compared among groups using the one-way ANOVA test for *in vitro* experiments and two-way ANOVA test for *in vivo* experiments, followed by the

Tukey's or Dunnett's post-test depending on the experiment. The difference between groups was considered significant when p-value <0.05 (*), <0.01 (**), <0.001 (***) or <0.0001 (****).

3 Results and Discussion

3.1 Synthesis of PNVP Derivatives

To impart amphiphilicity to PNVP and allow its anchoring into the membrane of the lipoplexes, this hydrosoluble polymer sequence was end-functionalized with different hydrophobic groups, namely OD, DiOD and DSPE. The general synthesis strategy, shown in **Figure 2**, involves the RAFT polymerization [37,38], a tool of choice for the preparation of well-defined functional polymers of interest for biomedical applications, in particular PNVP-based materials [39,40].

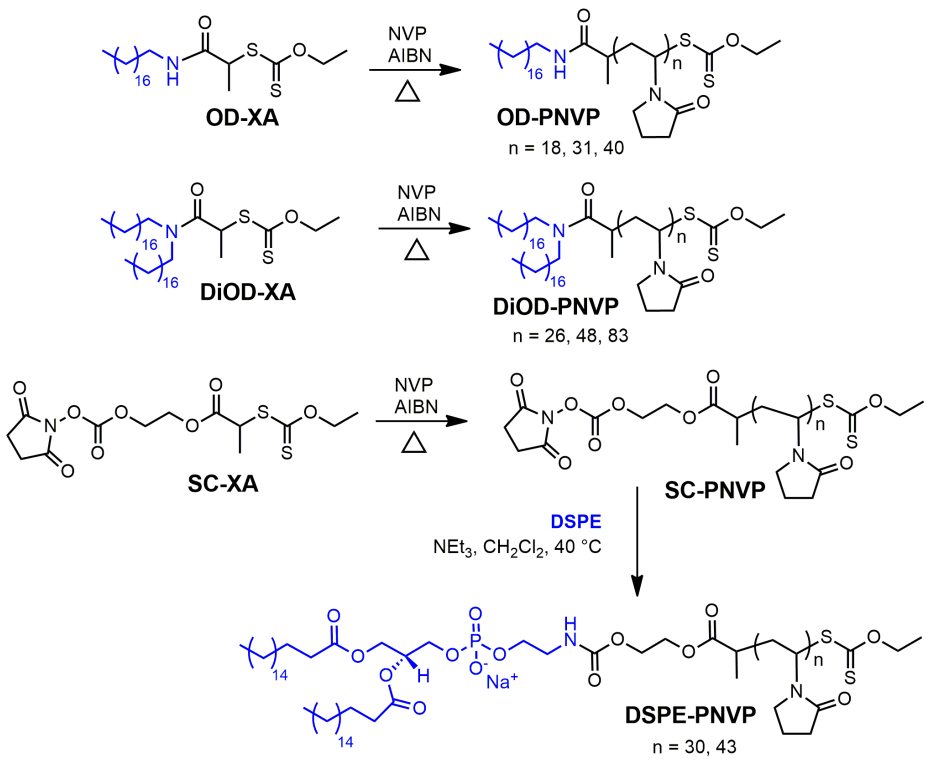

Figure 2: General strategy for the synthesis of the amphiphilic PNVP derivatives.

Briefly, various OD-PNVP and DiOD-PNVP compounds were produced via RAFT polymerization of NVP using octadecyl- or dioctadecyl-functional xanthates (OD-XA and DiOD-XA) as chain transfer agents. The synthesis of the DSPE-PNVP derivatives was achieved by a two step-process based on (i) RAFT of NVP initiated by a xanthate containing a succinimidyl carbonate (SC-XA) and (ii) coupling of the resulting succinimidyl carbonate-PNVP (SC-PNVP) with the amino group of DSPE. The DP of PNVP and so the molar mass of the hydrophilic part, was adjusted by the monomer/RAFT agent ratio. **Table 1** summarizes the PNVP structures prepared accordingly and tested to decorate lipoplexes in the next sections. Synthesis and characterization of the PNVP compounds are detailed in the SI (**Schemes S1-S4, Tables S1-S4, Figures S1-S3**). All polymers were purified by repeated precipitation, prolonged dialysis in water and lyophilization. In agreement with previous studies [41], this treatment induced the hydrolysis and removal of the terminal xanthate as confirmed by the ^{1}H NMR analysis (**Figures S1-S3**). In the case of DSPE-$PNVP_{30}$, the XA removal was achieved by treatment with lauroyl peroxide (LPO) at 80 °C in isopropanol as reported by Destarac *et al.* [42,43] (**Figure S4A**). Proper elimination of the XA terminal group of DSPE-$PNVP_{30}$ was confirmed by the disappearance of the xanthate characteristic absorption peak at 290 mm in the size exclusion chromatography-UV curves (**Figure S4B**).

Table 1. Characteristics of the PNVP derivatives.

Polymer	DP[a]	$M_{n\ NMR}$ [b] (g/mol)	$Đ$ [c]
Et-PNVP$_{19}$	19	2100	1.14
OD-PNVP$_{18}$	18	2000	1.19
OD-PNVP$_{31}$	31	3400	1.21
OD-PNVP$_{40}$	40	4400	1.32
DiOD-PNVP$_{26}$	26	2900	1.21
DiOD-PNVP$_{48}$	48	5300	1.21
DiOD-PNVP$_{83}$	83	9200	1.23
DSPE-PNVP$_{43}$	43	4800	1.14
DSPE-PNVP$_{30}$	30	3300	1.18

[a] Degree of polymerization of PNVP calculated based on the $M_{n\ NMR}$. [b] M_n of PNVP determined by ^{1}H NMR. [c] Determined by SEC DMF/LiBr with a PS calibration.

3.2 Physicochemical Properties of Grafted Lipoplexes

The post-insertion of the amphiphilic polymers into lipoplexes was evaluated by measuring several physicochemical properties of post-grafted lipoplexes (size, PdI, charge (Zp) and encapsulation efficiency) compared to naked lipoplexes (**Figure 3**). Et-, OD-, DiOD-, and DSPE-PNVP polymers were added in different proportions to the lipoplexes (10, 15, 30 and 40% to total lipids (%mol)). Et-PNVP is a polymer comprising an ethyl segment too short to confer amphiphilic properties and consequently insert into lipoplexes. Thus, no change in the physicochemical properties of lipoplexes is expected in the presence of the Et-PNVP. This polymer was used as a negative control while DSPE-PEG was used as a positive control.

The Z-average size of naked-lipoplexes was around 200 nm and did not further increase significantly with increasing amounts of the different polymers (**Figure 3A**). Although a trend of

decreasing size was observed with increasing polymer concentration, especially for the DSPE-PEG and DSPE-$PNVP_{43}$ polymers. For the DSPE-$PNVP_{43}$ lipoplexes (40%), the size was even significantly reduced compared to naked lipoplexes. The size of lipoplexes was therefore slightly affected by the addition of polymers except when large quantities of DSPE-$PNVP_{43}$ were added, a phenomenon also observed for DSPE-PEG.

The polydispersity index (PdI) of lipoplexes (below 0.1 for naked lipoplexes) increased significantly for DSPE-PNVP lipoplexes as well as for PEGylated lipoplexes (PdI > 0.2 at 10, 15, 30 and 40% of DSPE-PNVP and DSPE-PEG polymers), reflecting a higher heterogeneity of the dispersion after the post-insertion. OD- and DiOD-PNVP lipoplexes induced a non-significant increase of the PdI (0.1 - 0.2 at 15, 30 and 40%). Similar results have been previously described and attributed to their different conformations in function of quantities around the lipoplexes [30]. We showed that the PdI of grafted lipoplexes is mainly affected by the addition of polymers containing the hydrophobic DSPE segment (DSPE-PEG and DSPE-PNVP) which can be due to an effective insertion within the membrane of the lipoplexes (**Figure 3B**).

The surface charge (Zp) of all formulations was also evaluated (**Figure 3C**). PEGylation is known to reduce the surface charge of cationic liposomes [44] by masking the positive charges [30]. As expected, except for Et-PNVP lipoplexes, a decrease of the Zp was observed for all formulations compared to naked lipoplexes (around + 45 mV). At 40%, OD- and DiOD-PNVP lipoplexes showed a residual positive surface charge (between +10 and +30 mV) while DSPE-PNVP lipoplexes showed a negative Zp (around -15 mV) as observed with PEGylated lipoplexes. This difference can be explained by the negative charge of the DSPE segment. As expected, the treatment of lipoplexes with Et-PNVP did not change their surface charge suggesting a poor anchoring of this polymer at the surface of the carrier. By contrast, the decrease of the surface

charge observed for the other formulations might indicate that OD-, DiOD- and DSPE-PNVP polymers are present on the lipoplexes surface and, at least partially, mask their surface charge.

The effect of polymer grafting on siRNA complexation efficiency was evaluated. Naked lipoplexes showed a complexation rate higher than 90%. The complexation rate remained close to 88% for Et-, OD- and DiOD-PNVP lipoplexes, whatever the percentage and the length of the hydrophilic chain. This contrasts with the complexation rate observed with DSPE-PNVP and DSPE-PEG lipoplexes for which the complexation efficiency of siRNA dropped to around 45% in the presence of 40% of these polymers, regardless of the hydrophilic chain length (**Figure 3D)**. Interestingly, similar results were previously observed with PEGylated lipoplexes. Hattori *et al.* also observed an increase in the free siRNA fraction for PEGylated lipoplexes [12]. The decrease in siRNA complexation could be explained by a partial release of the encapsulated siRNA due to DSPE-based polymers insertion into the lipoplexes. Post-treatment of the lipoplexes with Et-, OD- and DiOD-PNVP, however, did not disturb the encapsulation of siRNA which might suggest that the latter do not efficiently insert into lipoplexes in contrast to their DSPE counterparts. This hypothesis was confirmed by NTA analyses showing more complex size distribution profiles when lipoplexes were grafted with DSPE-PNVP or DSPE-PEG polymers (15%) (**Figure 3G-H**) compared to naked lipoplexes or lipoplexes to which OD-PNVP polymers were added (**Figure 3E-F**).

No significant impact of the hydrophilic chain length on size, PdI, surface charge and encapsulation efficiency was observed.

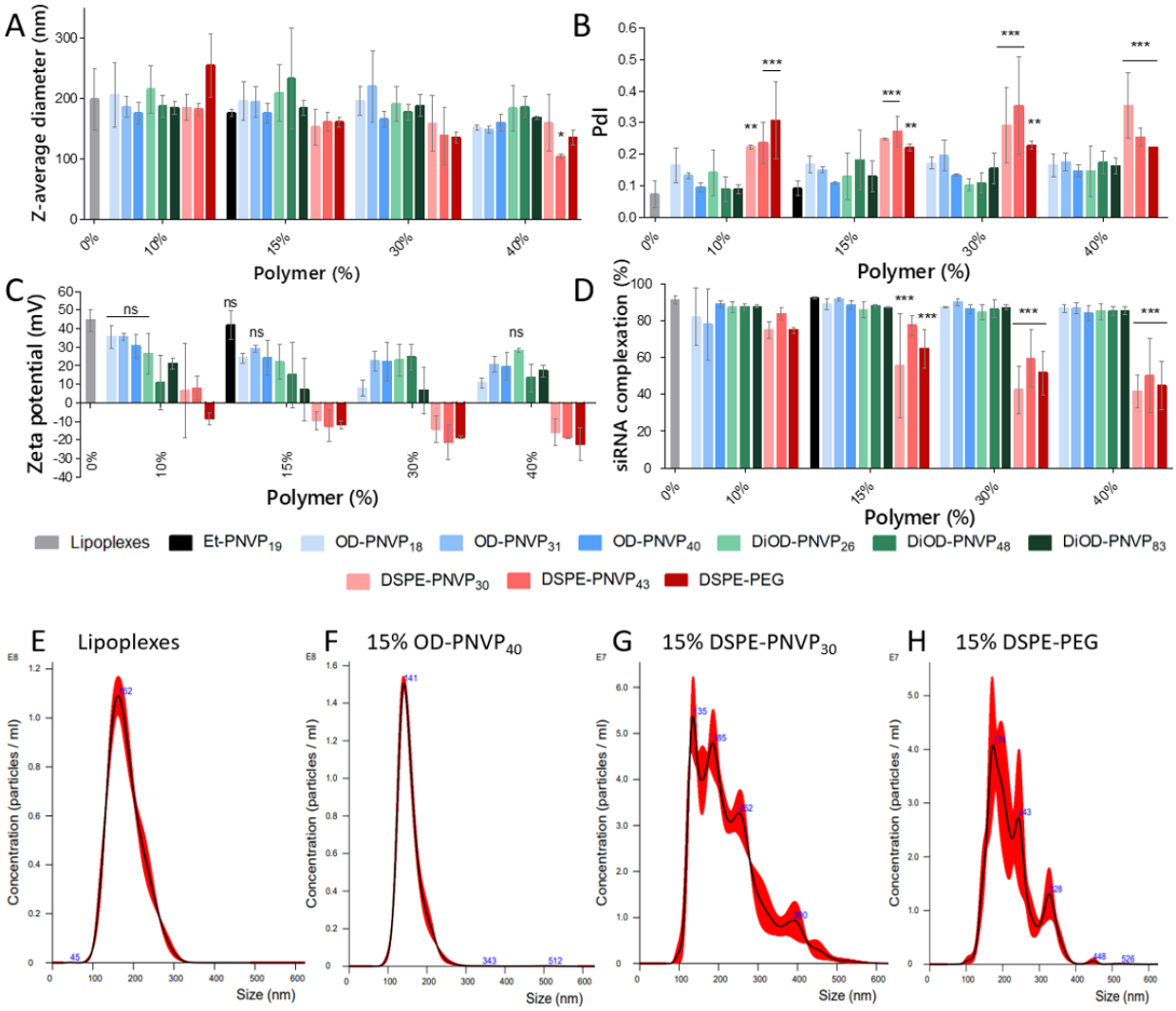

Figure 3: Impact of lipoplex (N/P 2.5, 100 nM) post-grafting with increasing percentages (0, 10, 15, 30, 40% molar ratio of total lipids) of polymers on physicochemical properties: Z-average diameter (nm) (**A**), PdI (**B**), Zeta Potential (Zp) (mV) (**C**) and siRNA complexation (%). Each value represents the mean +/- standard deviation (SD) of three independent experiments (n=3). Statistical analyses were performed by one-way ANOVA, followed by the Tukey's test. (**D**). Particle distribution profiles given by NTA of (**E**) naked lipoplexes or lipoplexes grafted with 15% (**F**) OD-PNVP$_{40}$, (**G**) DSPE-PNVP$_{30}$ and (**H**) DSPE-PEG.

To gain insight into the interactions of the different PNVP derivatives with lipoplexes, we monitored their binding with a model lipid bilayer via quartz crystal microbalance with dissipation analysis (QCM-D). The liposome membrane was mimicked by a supported lipid bilayer (SLB) consisting of DOTAP/Chol/DOPE deposited onto gold coated quartz crystals by a procedure

adapted from literature [33,34] (**Figure S5**). The SLB was then exposed to a continuous flow of polymer solutions (30 µM) and sensor frequency changes due to polymer binding were converted into deposited masses according to the Sauerbrey equation [45,46] ($\Delta m = -C.\Delta f/n$) (**Figure 4**). No frequency change was observed for Et-PNVP confirming the absence of membrane interaction in case of PNVP compounds deprived of long aliphatic chain (**Figure 4A**). A sharp decrease in frequency ($\Delta f \sim 9$ Hz) was observed upon OD-PNVP addition followed by a marked increase in frequency during the final rinse highlighting a weak anchoring of this polymer within the SLB (**Figure 4B**). For DiOD-PNVP, Δf only reached 2 Hz corresponding to 5 $ng.cm^{-2}$ but the deposited mass density was preserved during washing (**Figure 4C**). Finally, a classical adsorption profile was recorded for DSPE-PNVP with a gradual decrease in frequency until $\Delta f \sim 9$ Hz corresponding to 23 $ng.cm^{-2}$ (**Figure 4D**). Importantly, the deposited mass was maintained during the final rinsing demonstrating the efficient binding of DSPE-PNVP. An increase of dissipation ($\Delta D > 0$) was also measured in line with a softer surface structure due to the presence of a hydrated PNVP layer onto the SLB (**Figure S6b**). Finally, curves of the different quartz crystal overtones (from 5 to 13^{th}) mostly overlapped confirming the insertion of DSPE-PNVP within the SLB rather than the simple deposition on the upper surface of the latter (**Figure S6a**) [34].

In summary, Et-PNVP, OD-PNVP and DiOD-PNVP showed inexistent, transient, and limited interaction with the DOTAP/Chol/DOPE membrane, respectively, whereas efficient binding was achieved with DSPE-PNVP.

These observations corroborated the DLS, Zp and NTA measurements, suggesting a significant change in the structure and charges of the lipoplexes, essentially for DSPE-PNVP, and that the grafting of polymers containing a DSPE moiety occurs in a different and more efficient manner than those containing OD or DiOD chains.

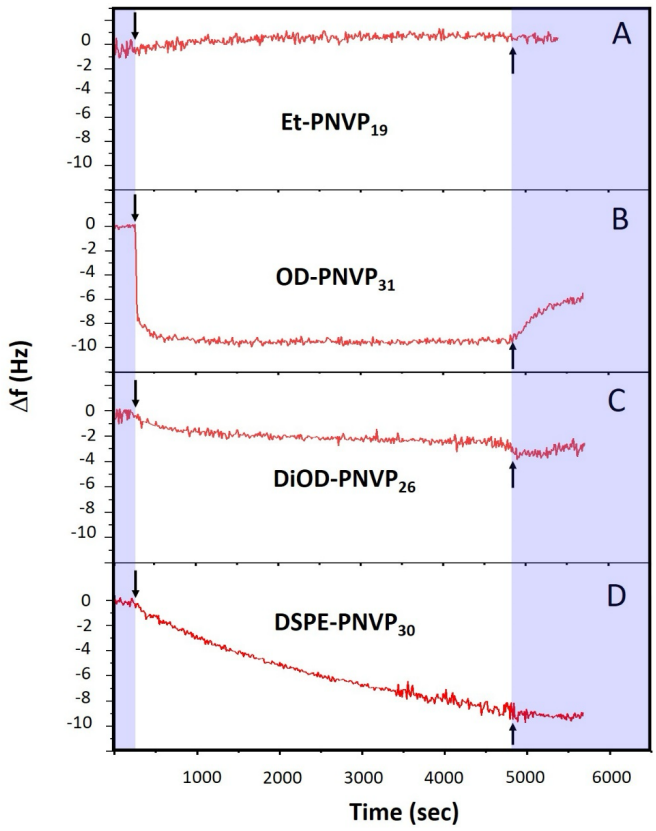

Figure 4: Δf traces (7th harmonic) from QCM-D monitoring of the deposition of (A) Et-PNVP$_{19}$, (B) OD-PNVP$_{31}$, (C) DiOD-PNVP$_{26}$ and (D) DSPE-PNVP$_{30}$ at a concentration of 30 µM on DOTAP/Chol/DOPE (1/0.75/0.5 molar ratio) membranes at 25°C. The arrows designate the polymer solution addition (arrow down) and the final rinsing with buffer (arrow up). Blue regions correspond to buffer elution periods.

3.3 Formation of the Protein Corona

Figure 5A and 5B show the increase in lipoplex mean size observed after 2 h of incubation in HI FBS. For naked lipoplexes, the formation of a protein corona resulted in changes in the distribution profile characterized by an increase in particle mean size (shift of the curve towards larger size) (**Figure 5A**). The same observation was made for Et-, OD- and DiOD-PNVP lipoplexes. On the contrary, DSPE-PNVP and DSPE-PEG lipoplexes showed less disturbed and more superimposed size distribution profiles compared to the initial profile, showing that the adsorption of FBS

proteins was strongly reduced. As explained above, the profiles of DSPE-PEG and DSPE-PNVP lipoplexes were already disrupted at T_0 due to the insertion of the polymers into the lipoplexes but thereafter they were less disrupted in presence of FBS (**Figure 3G-H**). These observations confirm that DSPE-PEG and DSPE-PNVP were effective in preventing protein corona formation around the lipoplexes. Although it was difficult to confirm the maintenance of a constant particle size over time due to the more dispersed distribution of lipoplexes containing 15% DSPE-PNVP or 15% DSPE-PEG, it was possible to use the average particle size by monitoring individual particles (NTA). By comparing the average size before and 2 hours after the addition of FBS, the formation of the protein corona could be assessed (**Figure 5B)**. For Et-, OD-, and DiOD-PNVP lipoplexes, a similar size increase to naked lipoplexes was observed (about 100 nm), independently of the hydrophilic chain length. Below 15% of DSPE-PNVP or DSPE-PEG, the increase in the mean size of lipoplexes was not significantly different from that of naked lipoplexes, demonstrating comparable adsorption of proteins around the lipoplexes. In contrast, when DSPE-PNVP and DSPE-PEG are used at a concentration of at least 15%, the increase in average particle size is significantly reduced compared with that of naked lipoplexes. For DSPE-PNVP polymers, a minimum amount of 15% was necessary to effectively avoid an increase in lipoplex size and thus avoid the formation of the protein corona as also observed with 15% DSPE-PEG.

These results confirmed the importance of the DSPE segment to efficiently insert into the lipoplexes and consequently protect particles from the formation of the protein corona.

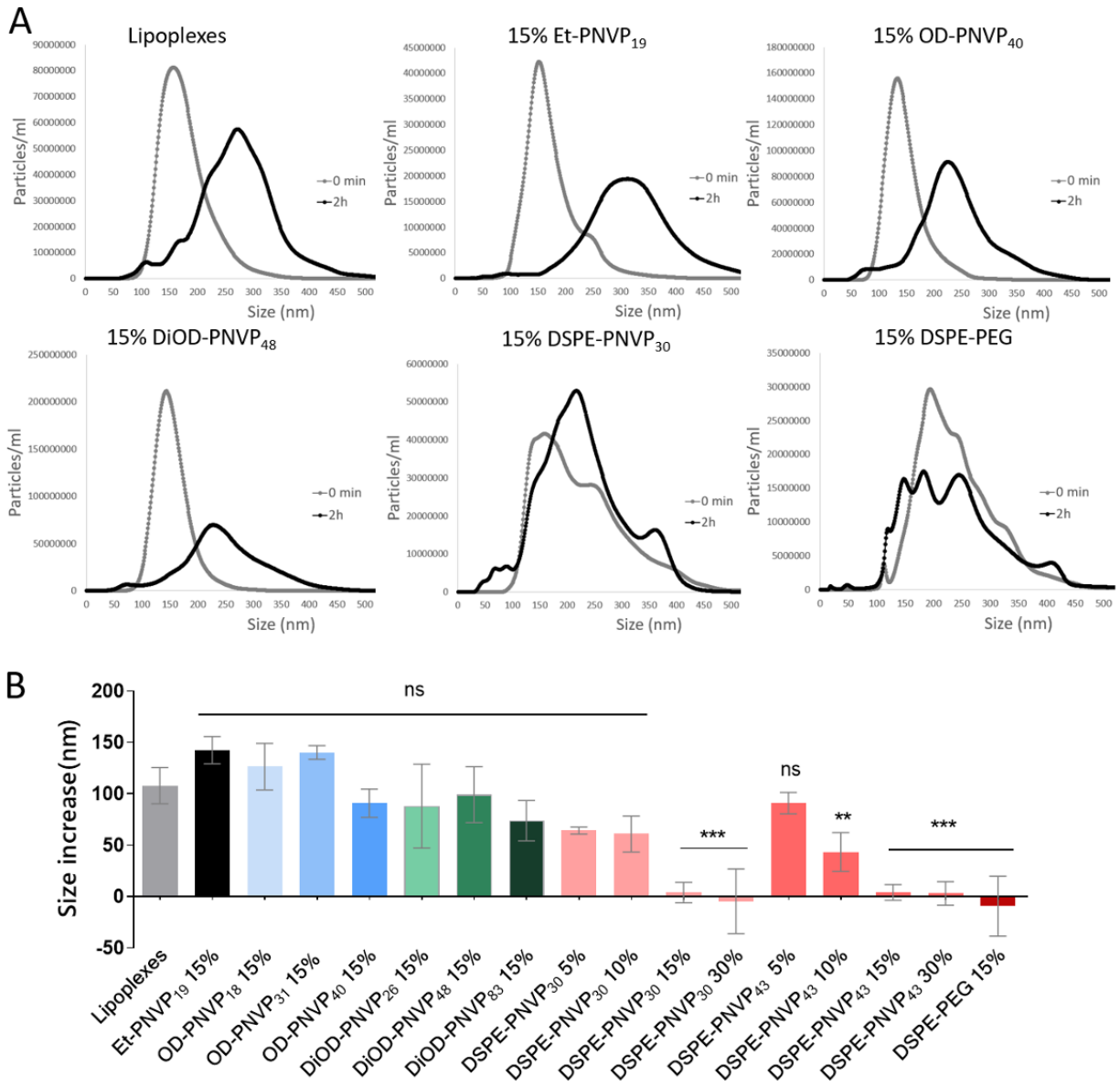

Figure 5: (**A**) Particle size (in nm) distribution profiles obtained before and after 2 h of incubation in heat-inactivated (HI) serum (33.33% v/v) (respectively in grey and black) using the NTA method. (**B**) Increase in the lipoplex mean size after 2 h in HI FBS (measured using the NTA method). Each value represents the mean +/- standard deviation (SD) of three independent experiments (n=3). Statistical analyses were performed by one-way ANOVA, followed by the Tukey's test.

3.4 Evaluations of Toxicity

3.4.1 Toxicity of Polymers and Post-grafted Lipoplexes *in cellulo*

The toxicity of polymers alone was first evaluated *in cellulo* using MTT assay. A549 cells were treated with different amounts of polymers up to a molar ratio of 150. Except for OD-PNVP$_{18}$ and DiOD-PNVP$_{48}$, all polymers did not show cell mortality (> 80% of viable cells after 24 h of treatment) and were comparable to DSPE-PEG for all tested amounts (**Figure 6A**).

Next, cell viability was assessed with grafted lipoplexes containing irrelevant siGL3 **(Figure 6B**). A slight decrease in cell viability (≈10%) was observed for cells treated with naked lipoplexes. A significant decrease in cell viability (≈ 40%) was also observed with all grafted lipoplexes. However, it is important to note that the viability remained comparable between cells treated with DSPE-PEG lipoplexes and those treated with PNVP lipoplexes. Because MTT assay cannot discriminate between cell death *per se* (cytotoxicity effect) and reduction in cell proliferation (cytostatic effect), an apoptosis assay was next performed. A549 cells were treated with grafted lipoplexes. No significative increase in apoptotic cell death was observed after incubation with all formulations (**Figure 6C**). In addition, microscopic observations of cells showed no presence of floating dead cells after treatment with all tested PNVP lipoplexes even after prolonged incubation period (data not shown). These results suggest that decrease in cell viability observed by MTT assay after treatment with PNVP lipoplexes is likely related to reduction of cell proliferation, and not due to an increase in apoptotic cell death.

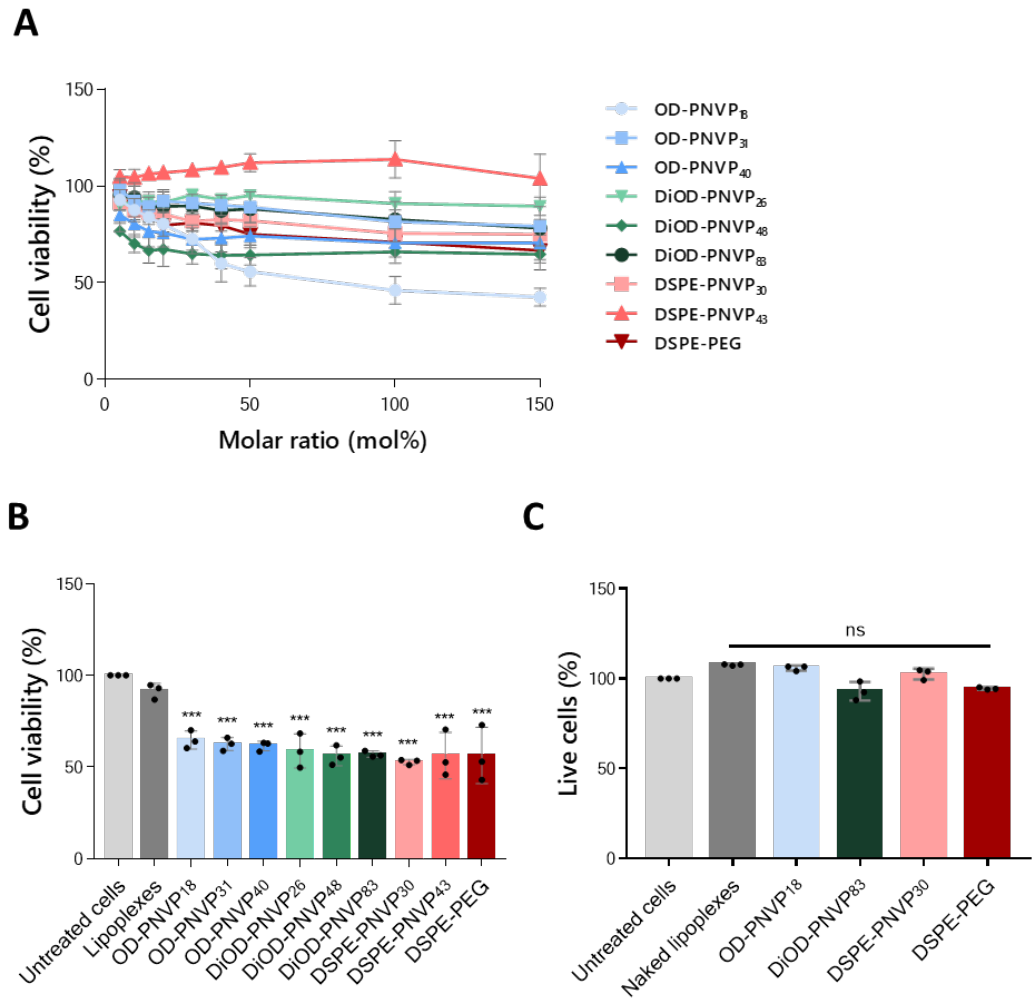

Figure 6: Cell viability of A549 cell line treated for 24 h with (**A**) polymers at various amounts (molar ratio compared to the total of lipid, from 5 to 150) and (**B**) lipoplexes or grafted lipoplexes determined using MTT cell viability assay. ($p = 0.6548$ for Lipoplexes; $p < 0.001$ for OD-PNVP$_{18}$, OD-PNVP$_{31}$, OD-PNVP$_{40}$, DiOD-PNVP$_{26}$, DiOD-PNVP$_{48}$, DiOD-PNVP$_{83}$, DSPE-PNVP$_{30}$, DSPE-PNVP$_{43}$ and DSPE-PEG). (**C**) Percentage of live cells incubated for 24 h with lipoplexes or grafted lipoplexes measured using Annexin V-FITC/PI apoptosis assay ($p = 0.3295$ for Lipoplexes, $p > 0.9999$ for OD-PNVP$_{18}$, $p = 0.8389$ for DiOD-PNVP$_{83}$, $p > 0.9999$ for DSPE-PNVP$_{30}$ and $p > 0.9999$ for DSPE-PEG). Each value represents the mean +/- standard deviation (SD) of three independent experiments (n=3). For MTT test, each independent experiment represents the mean of a quadruplicate. Statistical analyses were performed using a one-way ANOVA test where each group was compared to the group untreated cells.

3.4.2 Toxicity in a Zebrafish Model

We then tested the toxicity of the DSPE-PNVP lipoplexes on Zebrafish which became a widely used model to elucidate the *in vivo* behavior (toxicity, biodistribution, pharmacokinetic, therapeutic effect) of nanoparticles. The zebrafish model is currently commonly used to determine the toxicity of a drug in the early stages of a study. Indeed, because of the transparency of the embryos, it is possible to investigate the cause of toxicity with a cost-effective, rapid and high fidelity method. Moreover, with about 70% of genes in common with humans, the zebrafish model can be used as a predictive tool. Changes in organ size or shape, or impact on embryonic development will be an indicator of biological toxicity [47–50].

After 2 doses, no specific toxicity was observed compared to the control as shown in **Figure 7.** The morphology of embryos looked normal at any concentration tested: non-curved tail or body axis deformation, no pericardial or yolk sac edema, normal embryonic development compared with the control. Based on these results, it can be concluded that the DSPE-PNVP lipoplexes are not toxic in these live organisms.

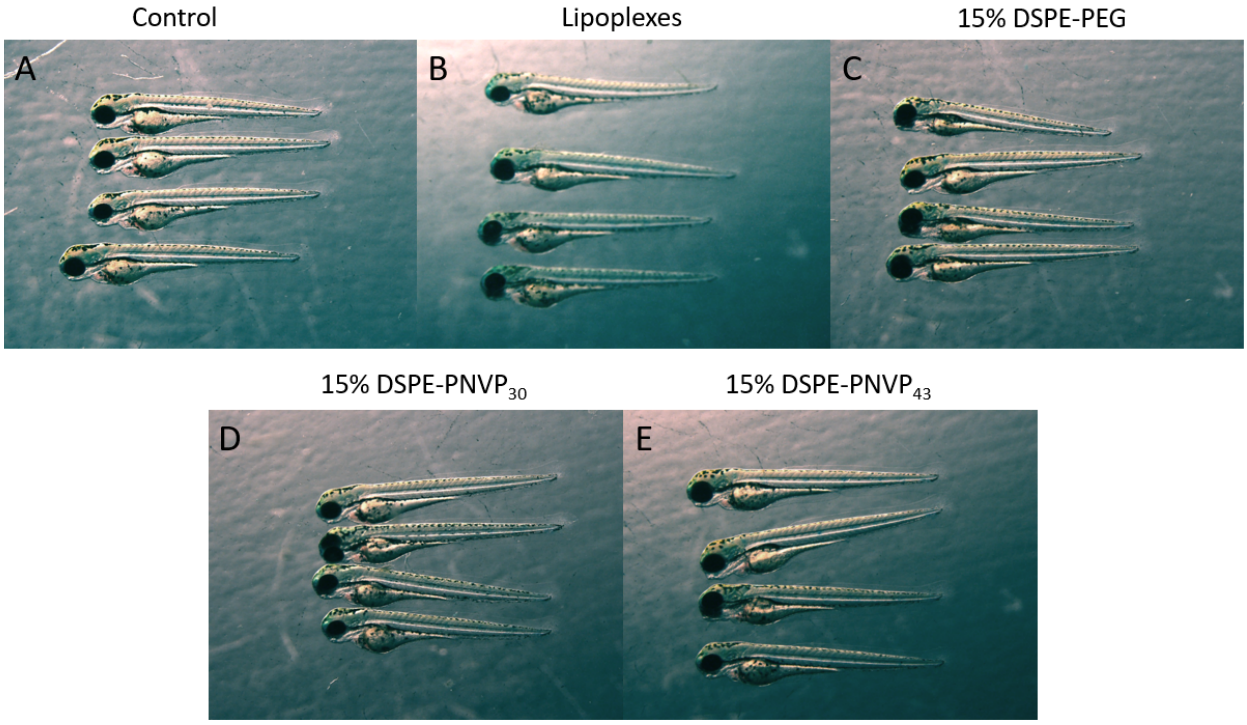

Figure 7: Assessment of lipoplex (100 nM siGL3) toxicity in Zebrafish model after two administrations at 10g siRNA/kg (72 hpf) compared with control condition. (**A**) Control (**B**) Naked lipoplexes (**C**) PEGylated lipoplexes (**D**) DSPE-PNVP$_{30}$ lipoplexes(**E**) DSPE-PNVP$_{43}$ lipoplexes.

3.4.3 Impact on Human Normal Blood Function

To plan parenteral administration, the blood biocompatibility of lipoplexes was evaluated. Compared with the control (Triton X-100), all lipoplex formulations (OD-, DiOD-, and DSPE-PNVP/PEG lipoplexes (15%)) did not show a significant hemolytic (**Figure 8A**) or platelet aggregation effect (**Figure 8B**).

All these results suggest the safe use of these formulations as a PEG alternative.

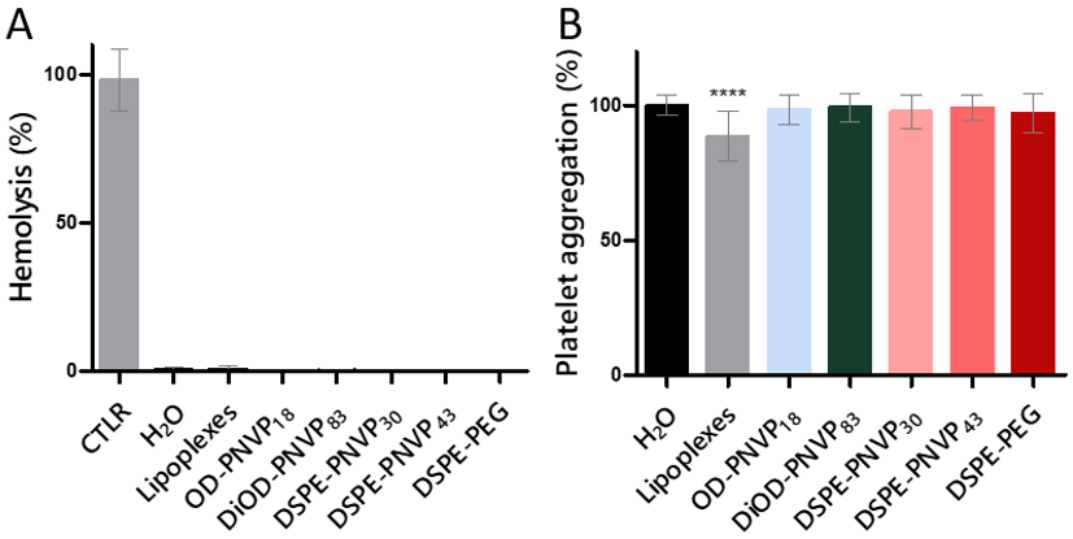

Figure 8: Hemocompatibility assays of lipoplexes and grafted lipoplexes (15% polymer), performed at a final concentration of siGL3 of 200 nM. (**A**) Human RBC lysis (% of hemolysis) in whole blood after 1 h incubation with formulations at 37°C. Triton X-100 1% is used as a positive control. (**B**) Platelet aggregation induced by collagen in the presence of the different formulations. H_2O is used as negative control. Results are expressed as % of response, normalized to H_2O. Each value represents the mean +/- standard deviation (SD) of three independent experiments (n=3). Statistical analyses were performed by using one-way ANOVA, followed by the Dunnett's post-test.

3.5 Cell uptake and Gene Silencing

One critical step for an efficient gene silencing is the siRNA internalization and release. This step is considered as one of the most important limitations of PEGylated lipoplexes as polymer grafting is known to reduce interactions with cell membranes and subsequently decrease cellular uptake and endosomal escape preventing siRNA delivery and gene silencing [51–54].

3.5.1 Cell Uptake

To evaluate the capacity of grafted lipoplexes to cross the cell membrane and gain access to cytoplasm, the intracellular fluorescence intensity of labeled-Cy5 GL3 siRNA-lipoplexes was measured. As shown in **Figure 9A**, compared to naked lipoplexes, the cell internalization of lipoplexes was reduced by about 80% after the grafting of DSPE-PEG on their surface. This observation is consistent with the well-known *PEG dilemma* [30,44,55–57]. Compared with naked

lipoplexes, the presence of OD- and DSPE-PNVP polymers did not reduce the amount of internalized fluorescent siRNA. For DiOD-PNVP lipoplexes, cellular penetration seemed to be dependent on the length of the hydrophilic chain. Indeed, the intracellular fluorescence intensity decreased with short hydrophilic chain. A lower uptake was observed when cells were treated with lipoplexes post-inserted with DiOD-PNVP$_{26}$ and DiOD-PNVP$_{48}$ compared with DiOD-PNVP$_{83}$ lipoplexes. This effect was almost comparable to the one observed for DSPE-PEG lipoplexes. Finally, lipoplexes grafted with DSPE-PNVP$_{30}$ and DSPE-PNVP$_{43}$ were able to penetrate approximately 4 and 5-fold more efficiently than the DSPE-PEG lipoplexes, respectively. Thus, for the majority of DSPE-PNVP lipoplexes, the cell uptake is higher than that of DSPE-PEG lipoplexes.

3.5.2 Gene Silencing Efficiency

The next step of the proof-of-concept is to evaluate the impact of the polymer on lipoplex gene silencing efficiency. To address this question, A549 cells stably expressing GFP were used and the ability of naked lipoplexes and grafted lipoplexes to transfect a siRNA against GFP (siGFP) was determined. The inhibition of the GFP fluorescence intensity is therefore an indicator of siRNA transfection efficiency, which combines cellular entrance, delivery/release, and degradation of target mRNA. We found that naked lipoplexes decreased the fluorescence by about 60% after 72 h. As expected, due to the *PEG dilemma*, PEGylated lipoplexes decreased the fluorescence less than naked lipoplexes (about 40%). OD-PNVP derivatives with different hydrophilic chain length did not significantly decrease the GFP fluorescence. Interestingly, DiOD- and DSPE-PNVP lipoplexes efficiently decreased the fluorescence (decrease of fluorescence comprised between 25% and 51%) (**Figure 9B).** The length of the hydrophilic chain length DiOD-PNVP seems to affect the siRNA transfection efficiency. Indeed, DiOD-PNVP$_{48}$ and DiOD-PNVP$_{83}$ lipoplexes

showed a significant decrease in GFP fluorescence while DiOD-$PNVP_{26}$ lipoplexes did not. This transfection efficiency seems to be correlated to the cell uptake as well. Indeed, the most internalized formulation (DiOD-$PNVP_{83}$ lipoplexes) was the most efficient to inhibit the GFP expression in cells. At the same time, the internalization of DiOD-$PNVP_{26}$ was the lowest of DiOD-PNVP grafted lipoplexes. Concerning DSPE-PNVP lipoplexes, an increase in the hydrophilic chain length tends to decrease the efficiency. Furthermore, with respect to the impact of the polymer percentage, the best polymer concentration seems to be 15% as higher percentage seems to have a negative effect. Our results seem to be consistent to what was observed with PEGylated liposomes. It is known that the efficacy of PEGylation mainly depends on two factors: (i) the chain length and (ii) the surface coverage density. PEG_{2000} polymer is widely used because it has an appropriate chain length. Indeed, short PEG (PEG_{750} or shorter) are not able to efficiently increase the liposome blood circulation time while longer PEG (PEG_{5000} or more) have a significant negative impact on cellular uptake and endosomal escape [58]. Moreover, higher coverage is obtained when a high molar ratio of PEG is used (total lipid ratio) and PEG molecules can adopt a brush-like configuration leading to a better steric barrier, but also greater prevention of gene delivery in tumor cells [13,44]. It seems that a similar *dilemma* can be observed with DSPE-PNVP and DSPE-PEG, as gene silencing appears to decrease when increasing the surface coverage density or/and chain length increase. Lipoplexes post-grafted with 15% DSPE-$PNVP_{30}$ or DSPE-PEG give similar gene delivery efficiency. As with DSPE-PEG, the chain length and surface coverage of DSPE-$PNVP_{30}$ could be a good compromise between the prevention of protein corona formation and efficient gene delivery.

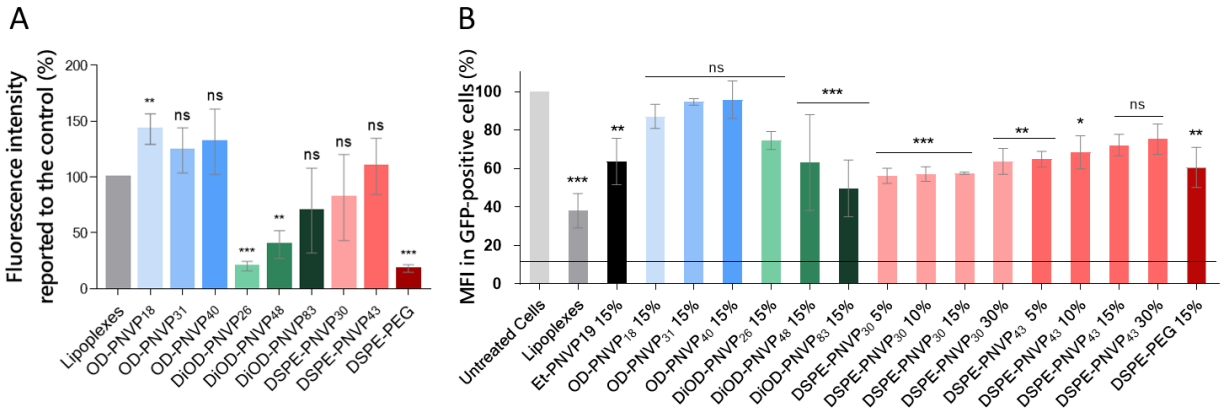

Figure 9: Effect of PNVP derivatives on (**A**) Cellular uptake of lipoplexes and grafted lipoplexes in A549 cells. Intracellular fluorescence intensity of siGL3 Cy5 was detected by flow cytometry after 4 h of incubation. Each value represents the mean +/- standard deviation (SD) of three independent experiments (n=3). Statistical analyses were performed using a one-way ANOVA test where each group was compared to cells treated with naked lipoplexes (group Lipoplexes) (p = 0.1726 for OD-PNVP$_{18}$, p = 0.7360 for OD-PNVP$_{31}$, p = 0.4573 for OD-PNVP$_{40}$, p = 0.0026 for DiOD-PNVP$_{26}$, p = 0.0265 for DiOD-PNVP$_{48}$, p = 0.5093 for DiOD-PNVP$_{83}$, p = 0.9047 for DSPE-PNVP$_{30}$, p = 0.9971 for DSPE-PNVP$_{43}$ and p = 0.0020 for DSPE-PEG). (**B**) Gene knockdown (MFI, %) in A549/GFP cells when transfected with lipoplexes carrying siGFP (100 nM) compared with naked lipoplexes, lipoplexes grafted with DSPE-PEG and with Lipofectamine® RNAiMAX (black line) after 72 h of transfection (n=3). Statistical comparisons with untreated cells were performed by one-way ANOVA, followed by the Tukey post-test.

3.6 *In vivo* Assay in Mice

Considering the physicochemical results, the low toxicity as well as the good internalization and efficiency to silence target mRNA, lipoplexes grafted with 15% DSPE-PNVP$_{30}$ were selected and compared with DSPE-PEG in immunocompetent BALB/c mice.

3.6.1 Biodistribution

To study the biodistribution and the ability to induce stealth properties, DSPE-PNVP$_{30}$ and DSPE-PEG lipoplexes coupled with fluorescent siGL3 Cy5.5 were intravenously injected twice (once a week). The fluorescence intensity of lipoplexes was monitored by *in vivo* imaging 5 h and 24 h post-injection. 5 h after the first and the second injection of DSPE-PEG or DSPE-PNVP$_{30}$ lipoplexes, a significant fluorescence intensity was detected in mice injected with both

formulations. After the second injection, the fluorescence observed 5 h later tends to be slightly higher than that observed after the first injection. 24 h after each injection, the fluorescence decreased, except for mice injected with DSPE-$PNVP_{30}$ lipoplexes that displayed a weak but significant fluorescent signal 24 h after the second injection (**Figures 10A**). The more rapid clearance of DSPE-PEG lipoplexes is likely related to the drastic accumulation of anti-PEG antibodies, which could form "antigen-antibody" complexes with newly administered PEGylated nanoparticles, leading to biodistribution/pharmacokinetic changes and accelerated organism elimination. Such important elevation of anti-PEG antibodies levels upon repeated injections of PEGylated lipoplexes could pose a real challenge for individuals by inducing severe adverse reactions such as hypersensitivity reactions. These results suggest that there is less ABC effect for DSPE-$PNVP_{30}$ lipoplexes.

A post-mortem investigation of the biodistribution of DSPE-PEG and DSPE-$PNVP_{30}$ lipoplexes, was performed on mice's organs including liver, spleen, heart, lung, and kidney. The quantification of the fluorescence intensity showed a high signal of Cy5.5 of DSPE-PEG and DSPE-$PNVP_{30}$ lipoplexes in kidney. A weak fluorescence was also detected in the heart whereas the other organs (liver, lung, and spleen) were completely negative (**Figures 10B and 10C**). The absence of hepatic accumulation for both formulations suggests good stealth properties of both DSPE-PEG and DSPE-PNVP lipoplex formulations, which do not seem to be cleared by the MPS (mononuclear phagocyte system). However, both lipoplex formulations were found to be mainly trapped in the kidney suggesting nanoparticles-kidney interactions and renal clearance. The abilities of DSPE-PEG and DSPE-$PNVP_{30}$ lipoplexes to either fully experience renal clearance or accumulate in certain parts of the kidney probably rely on a combination of various physicochemical characteristics such as their diameters, surface charge, structural properties, morphology.

3.6.2 Immune response: assessment of IgM and IgG production and proinflammatory cytokines

Natural or synthetic nanoparticles, depending on their characteristics and compositions, can interact with the immune system and therefore may modulate immune system function. Soluble mediators, such as antibodies (e.g. IgG, IgE, IgM) and cytokines, are often measured to predict immunomodulatory effects of nanomaterials and the possibility of inflammation-mediated toxicity [59].

IgM are mainly produced in the early phase after the first exposure to an antigen and are rapidly replaced by IgG, which represents a later-stage response and ensures long-term humoral response. To assess the presence of anti-polymers (anti-PEG and anti-PNVP) antibodies and give an overview of their time evolution after repeated administrations, we measured IgG and IgM levels 7 days post first and second dose injection using ELISA assay. **Figure 10D** shows the serum levels of anti-PEG IgG and anti-PEG IgM antibodies, seven days after each dose, compared with PBS injection used as a control. We observed the production of anti-PEG IgM after the first injection, confirming that the first administration of PEG-NPs stimulates responses by host immune systems. This level of anti-PEG IgM further increased after the second administration, with around 3-fold induction compared to the first injection. DSPE-PEG lipoplexes also induce production of anti-PEG IgG, which is also further increased after the second injection. The enhancement and longer lasting time of both anti-PEG IgM and IgG upon the second injection implies that an immune memory likely occurs.

Regarding anti-PNVP antibodies, we observed the accumulation of both anti-$PNVP_{30}$ IgM and IgG after the first injection of DSPE-$PNVP_{30}$ lipoplexes. More importantly, no increase of circulating anti-$PNVP_{30}$ IgM and IgG was observed after the second administration. The level of IgM and IgG against DSPE-$PNVP_{30}$ was even slightly decreased compared with the first injection. This time

course analysis of anti-PNVP IgG and anti-PNVP IgM demonstrated that no significant booster effect was observed after repeated administrations. Compared to DPSE-PEG, PNVP-grafted lipoplexes fail to generate boostable immune memory responses. These results therefore suggest that PNVP exhibit less potent immunogenicity than do PEG.

As stated above, studies have reported that nanoparticles can trigger cytokines production, which is associated with inflammatory responses. The levels of proinflammatory cytokines are often measured as biomarkers of nanoparticle immunomodulatory effects and immune-mediated toxicity [59]. Therefore, we investigated the effect of DSPE-PEG or DSPE-$PNVP_{30}$ on the systemic production of two most common pro-inflammatory cytokines (TNFα, IL-1β) after the two rounds of intravenous injection. As shown in **Figures 10F and 10G**, no increase in the level of IL-1β and TNF-α was detected in the serum of mice injected with DSPE-PEG lipoplexes or DSPE-$PNVP_{30}$ lipoplexes compared to the PBS control group. This result indicates that the intravenous administration of these grafted lipoplexes did not induce systemic inflammation-related responses *in vivo*. In accordance with the lack of toxicity *in vitro,* on human blood and in *in vivo* zebrafish model, these results demonstrated the safety of DSPE-$PNVP_{30}$ lipoplexes for *in vivo* applications.

Based on these results, PNVP-modified liposomes or lipoplexes could be proposed for the chronic administration of various active molecules, including siRNAs. Since DSPE-$PNVP_{30}$ grafted nanoparticles exhibited a weaker immune response *in vivo* compared to PEGylated lipoplexes, we can assume that the ABC effect could be minimized. This would allow lipoplexes to have an extended circulation time and accumulate more effectively at the target site, which is particularly crucial in the context of tumor accumulation. In addition, we were able to show that the use of 15% DSPE-PNVP prevented the nanoparticles from interacting with plasma proteins, thus avoiding the formation of the protein corona. This effect should guarantee stealth properties identical to those

observed with DSPE-PEG grafted nanoparticles, which will further increase the elimination half-life and therefore guarantee a long-term pharmacokinetics. This approach opens up promising perspectives for more effective therapies in the treatment of challenging diseases like cancer. As another reported limitation associated with the use of PEG is the risk of severe immune reactions, replacing the PEG polymer with PNVP derivatives, which offer similar benefits but have lower immunogenicity, could contribute to safer treatments or vaccinations [60]. The increasing number of patients with anti-PEG antibodies who have been previously exposed to PEGylated products (such as cosmetics, food and pharmaceuticals) underlines the importance of this approach.

4 Conclusion

A library of PNVP compounds with tunable hydrophilic and hydrophobic segments was generated with the goal to propose PEG alternatives for post-insertion modification of lipoplexes dedicated to efficient siRNA delivery associated with good stealth properties and less immune response. Amphiphilic polymers based on PNVP and single (OD) or dual aliphatic chains (DiOD), as well as DSPE as hydrophobic groups were synthesized.

Based on physicochemical properties and the efficiency in reducing protein corona formation, we observed that the DSPE segment is essential for the integration into the lipoplex structure by post-insertion. A similar gene silencing efficiency was observed for DSPE-$PNVP_{30}$ and for DSPE-PEG lipoplexes, confirming the famous PEG *dilemma* and that this *dilemma* also exists for DSPE-PNVP.

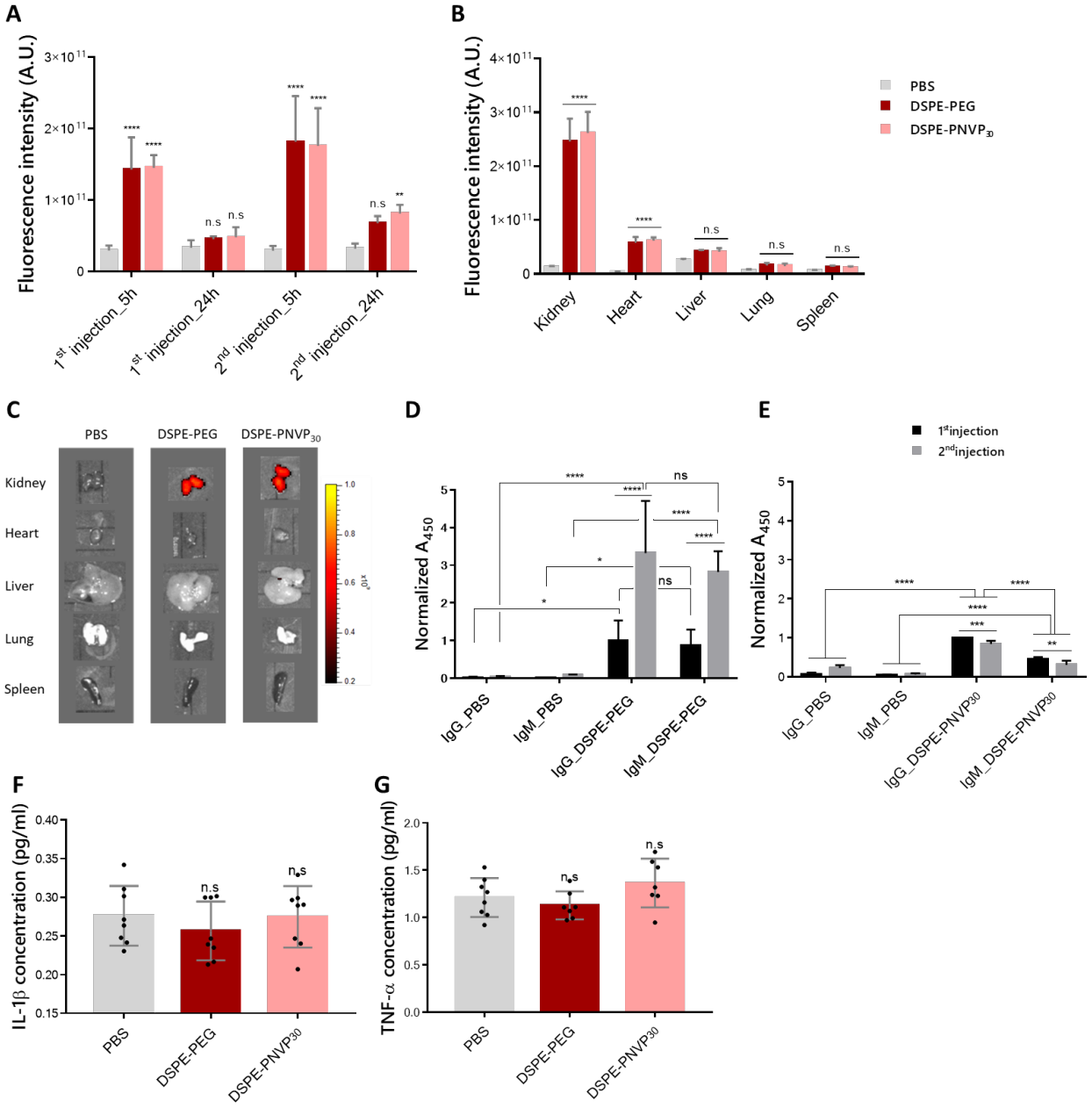

Figure 10: (**A**) Biodistribution of DSPE-PEG and DSPE-PNVP$_{30}$ lipoplexes detected using *in vivo* imaging. *In vivo* fluorescence intensity was measured after 5 h and 24 h of the first and the second intravenous injection ($p < 0.0001$ for DSPE-PEG and DSPE-PNVP$_{30}$ after 5 h of the 1st and the 2nd injection, $p = 0.6717$ for DSPE-PEG and $p = 0.5491$ for DSPE-PNVP$_{30}$ after 24 h of the 1st injection, $p = 0.0785$ for DSPE-PEG and $p = 0.002$ for DSPE-PNVP$_{30}$ after 24 h of the 2nd injection). The body accumulation of DSPE-PEG and DSPE-PNVP$_{30}$ lipoplexes prepared with siRNA GL3 Cy5.5 was detected by (**B**) measuring the fluorescence intensity ($p < 0.0001$ for DSPE-PEG and DSPE-PNVP$_{30}$ in kidney and heart, $p = 0.0903$ for DSPE-PEG in liver, $p = 0.1124$ for DSPE-PNVP$_{30}$ in liver, $p = 0.4593$ for DSPE-PEG in lung , $p = 0.5631$ for DSPE-PNVP$_{30}$ in lung, $p = 0.659$ for DSPE-PEG in spleen and $p = 0.7824$ for DSPE-PNVP$_{30}$ in spleen) using (**C**) *ex-vivo* fluorescence imaging in kidney, heart, liver, lung and spleen. The evolution of IgM and IgG

production in mice was detected using ELISA assay one week after the first and the second injection of **(D)** DSPE-PEG lipoplexes and (**E**) DSPE-$PNVP_{30}$ lipoplexes. Results were compared to a negative control group injected with PBS. *In vivo* toxicity of DSPE-PEG and DSPE-$PNVP_{30}$ lipoplexes was evaluated by detecting pro-inflammatory cytokines (**F**) IL-1β (p = 0.6105 for DSPE-PEG and p= 0.9842 for DSPE-$PNVP_{30}$) and (**G**) TNF-α (p = 0.6735 for DSPE-PEG and p = 0.3315 for DSPE-$PNVP_{30}$). Each value represents the mean +/- standard deviation (SD) of at least 7 mice (n = 7 or 8). For ELISA assay, the result of each mouse represents the mean of a duplicate. Statistical analyses were performed by two-way ANOVA test. In Figures A, B, F and G, results of the DSPE-PEG and DSPE-$PNVP_{30}$ groups were compared to that of the PBS group.

In vivo experiments in mice showed the absence of liver accumulation for both DSPE-PEG and DSPE-PNVP lipoplexes. A slight but significant extended circulation time was observed for the DSPE-PNVP lipoplexes 24 h after the second injection. The results demonstrated that DSPE-PNVP does not stimulate the production of IgM/IgG following repeated administration, suggesting a less potent immunogenicity than do PEG. The coating of the surface of the lipoplexes with PNVP likely avoids recognition by the immune cells, impairs the ABC phenomenon and subsequently prolong the blood circulation time of these lipoplexes. Furthermore, no systemic pro-inflammatory response was observed for these PNVP-grafted lipoplexes as evidenced by unaltered level of proinflammatory cytokines compared to control conditions.

For the first time, this study presents an innovative approach to replace lipid-PEG with an alternative based on lipid-PNVP, a non-toxic and biocompatible polymer. Our study demonstrated the potential biological impact of PNVP polymers for post-insertion modification of lipoplexes. DSPE-$PNVP_{30}$ displays good stealth properties, less immunological response and no immunotoxicity. With excellent *in vitro* and *in vivo* behaviors, DSPE-PNVP polymers could therefore be proposed as interesting alternatives to DSPE-PEG for the delivery of siRNA lipoplexes or other lipid nanoparticles. This study, which involved a complete screening of different lipid-

PNVPs to select the best formulation for *in vivo* studies, offers promising prospects for the delivery of siRNA and other active molecules, and will require further *in vivo* evaluation.

Acknowledgment

The research was supported by the Wallonia-Brussels Federation (grant for Concerted Research Actions, LIPEGALT project, ULiège). Authors would like to thank Luc Duwez and Olivier Nivelles (GIGA-Mouse facility, university of Liege) for their help in mice experiments. Our data of flow cytometry and toxicity in Zebrafish were obtained with the assistance of the GIGA-Flow Cytometry and GIGA-Zebrafish facilities of the university of Liege.

A.D. is FNRS Senior Research Associate. D.M is FNRS Research Associate. They thank FNRS for financial support. A.D. also thanks M. Destarac for fruitful discussion.

Conflict of interest

The authors declare that they have no conflict of interest.

5 References

[1] R. Verbeke, I. Lentacker, S.C. De Smedt, H. Dewitte, The dawn of mRNA vaccines: The COVID-19 case, J. Control. Release. 333 (2021) 511–520. https://doi.org/10.1016/j.jconrel.2021.03.043.

[2] L. Schoenmaker, D. Witzigmann, J.A. Kulkarni, R. Verbeke, G. Kersten, W. Jiskoot, D.J.A. Crommelin, mRNA-lipid nanoparticle COVID-19 vaccines: Structure and stability, Int. J. Pharm. 601 (2021) 120586. https://doi.org/10.1016/j.ijpharm.2021.120586.

[3] M. Berger, A. Lechanteur, B. Evrard, G. Piel, Innovative lipoplexes formulations with enhanced siRNA efficacy for cancer treatment: Where are we now?, Int. J. Pharm. 605 (2021). https://doi.org/10.1016/j.ijpharm.2021.120851.

[4] J. Rüger, S. Ioannou, D. Castanotto, C.A. Stein, Oligonucleotides to the (Gene) Rescue: FDA Approvals 2017–2019, Trends Pharmacol. Sci. 41 (2020) 27–41. https://doi.org/10.1016/j.tips.2019.10.009.

[5] B. Hu, L. Zhong, Y. Weng, L. Peng, Y. Huang, Y. Zhao, X.J. Liang, Therapeutic siRNA: state of the art, Signal Transduct. Target. Ther. 5 (2020). https://doi.org/10.1038/s41392-020-0207-x.

[6] M. Berger, M. Degey, J. Leblond Chain, E. Maquoi, B. Evrard, A. Lechanteur, G. Piel, Effect of PEG Anchor and Serum on Lipid Nanoparticles: Development of a Nanoparticles Tracking Method, Pharmaceutics. 15 (2023). https://doi.org/10.3390/pharmaceutics15020597.

[7] J.S. Suk, Q. Xu, N. Kim, J. Hanes, L.M. Ensign, PEGylation as a strategy for improving nanoparticle-based drug and gene delivery, Adv. Drug Deliv. Rev. 99 (2016) 28–51. https://doi.org/10.1016/j.addr.2015.09.012.

[8] Y. Sakurai, H. Hatakeyama, Y. Sato, M. Hyodo, H. Akita, H. Harashima, Gene silencing via RNAi and siRNA quantification in tumor tissue using MEND, a liposomal siRNA delivery system, Mol. Ther. 21 (2013) 1195–1203. https://doi.org/10.1038/mt.2013.57.

[9] K. Son, M. Ueda, K. Taguchi, T. Maruyama, S. Takeoka, Y. Ito, Evasion of the accelerated blood clearance phenomenon by polysarcosine coating of liposomes, J. Control. Release. 322 (2020) 209–216. https://doi.org/10.1016/j.jconrel.2020.03.022.

[10] V. Francia, R.M. Schiffelers, P.R. Cullis, D. Witzigmann, The Biomolecular Corona of Lipid Nanoparticles for Gene Therapy, Bioconjug. Chem. 31 (2020) 2046–2059. https://doi.org/10.1021/acs.bioconjchem.0c00366.

[11] V.H. Nguyen, B.J. Lee, Protein corona: A new approach for nanomedicine design, Int. J. Nanomedicine. 12 (2017) 3137–3151. https://doi.org/10.2147/IJN.S129300.

[12] Y. Hattori, K. Tamaki, S. Sakasai, K.I. Ozaki, H. Onishi, Effects of PEG anchors in PEGylated siRNA lipoplexes on in vitro gene-silencing effects and siRNA biodistribution in mice, Mol. Med. Rep. 22 (2020) 4183–4196. https://doi.org/10.3892/mmr.2020.11525.

[13] G.T. Kozma, T. Shimizu, T. Ishida, J. Szebeni, Anti-PEG antibodies: Properties, formation, testing and role in adverse immune reactions to PEGylated nano-biopharmaceuticals, Adv. Drug Deliv. Rev. 154–155 (2020) 163–175. https://doi.org/10.1016/j.addr.2020.07.024.

[14] J. De Vrieze, Suspicions grow that nanoparticles in Pfizer's COVID-19 vaccine trigger rare allergic reactions, Science (80-.). (2020). https://doi.org/10.1126/science.abg2359.

[15] T.T.H. Thi, E.H. Pilkington, D.H. Nguyen, J.S. Lee, K.D. Park, N.P. Truong, The importance of Poly(ethylene glycol) alternatives for overcoming PEG immunogenicity in drug delivery and bioconjugation, Polymers (Basel). 12 (2020). https://doi.org/10.3390/polym12020298.

[16] A.S. Abu Lila, K. Nawata, T. Shimizu, T. Ishida, H. Kiwada, Use of polyglycerol (PG), instead of polyethylene glycol (PEG), prevents induction of the accelerated blood clearance phenomenon against long-circulating liposomes upon repeated administration., Int. J. Pharm. 456 (2013) 235–242. https://doi.org/10.1016/j.ijpharm.2013.07.059.

[17] P.H. Kierstead, H. Okochi, V.J. Venditto, T.C. Chuong, S. Kivimae, J.M.J. Fréchet, F.C. Szoka, The effect of polymer backbone chemistry on the induction of the accelerated blood clearance in polymer modified liposomes, J. Control. Release. 213 (2015) 1–9. https://doi.org/10.1016/j.jconrel.2015.06.023.

[18] O.K. Nag, V. Awasthi, Surface engineering of liposomes for stealth behavior, Pharmaceutics. 5 (2013) 542–569. https://doi.org/10.3390/pharmaceutics5040542.

[19] Y. Luo, Y. Hong, L. Shen, F. Wu, X. Lin, Multifunctional Role of Polyvinylpyrrolidone in Pharmaceutical Formulations, AAPS PharmSciTech. 22 (2021). https://doi.org/10.1208/s12249-020-01909-4.

[20] J. Kopeček, J. Yang, Polymer nanomedicines, Adv. Drug Deliv. Rev. 156 (2020) 40–64. https://doi.org/10.1016/j.addr.2020.07.020.

[21] D. Hwang, J.D. Ramsey, A. V. Kabanov, Polymeric micelles for the delivery of poorly soluble drugs: From nanoformulation to clinical approval, Adv. Drug Deliv. Rev. 156 (2020) 80–118. https://doi.org/10.1016/j.addr.2020.09.009.

[22] M. Kurakula, G.S.N.K. Rao, Pharmaceutical assessment of polyvinylpyrrolidone (PVP): As excipient from conventional to controlled delivery systems with a spotlight on COVID-19 inhibition, J. Drug Deliv. Sci. Technol. 60 (2020) 102046. https://doi.org/10.1016/j.jddst.2020.102046.

[23] M. Kurakula, G.S.N. Koteswara Rao, Moving polyvinyl pyrrolidone electrospun nanofibers and bioprinted scaffolds toward multidisciplinary biomedical applications, Eur. Polym. J. 136 (2020). https://doi.org/10.1016/j.eurpolymj.2020.109919.

[24] W.B. Liechty, D.R. Kryscio, B. V. Slaughter, N.A. Peppas, Polymers for drug delivery

systems, Annu. Rev. Chem. Biomol. Eng. 1 (2010) 149–173. https://doi.org/10.1146/annurev-chembioeng-073009-100847.

[25] V.. Torchilin, T.. Levchenko, K.. Whiteman, A.. Yaroslavov, A.. Tsatsakis, A.. Rizos, E.. Michailova, M.. Shtilman, Amphiphilic poly-N-vinylpyrrolidones: synthesis, properties and liposome surface modification, Biomaterials. 22 (2001) 3035–3044. https://doi.org/10.1016/s0142-9612(01)00050-3.

[26] I.A. Yamskov, A.N. Kuskov, K.K. Babievsky, B.B. Berezin, M.A. Krayukhina, N.A. Samoylova, V.E. Tikhonov, M.I. Shtilman, Novel liposomal forms of antifungal antibiotics modified by amphiphilic polymers, Appl. Biochem. Microbiol. 44 (2008) 624–628. https://doi.org/10.1134/S0003683808060112.

[27] Y. Liu, X. Luo, X. Xu, N. Gao, X. Liu, Preparation, characterization and in vivo pharmacokinetic study of PVP-modified oleanolic acid liposomes, Int. J. Pharm. 517 (2017) 1–7. https://doi.org/10.1016/j.ijpharm.2016.11.056.

[28] A. Lechanteur, T. Furst, B. Evrard, P. Delvenne, P. Hubert, G. Piel, Development of anti-E6 pegylated lipoplexes for mucosal application in the context of cervical preneoplastic lesions, Int. J. Pharm. 483 (2015) 268–277. https://doi.org/10.1016/j.ijpharm.2015.02.041.

[29] A. Lechanteur, T. Furst, B. Evrard, P. Delvenne, G. Piel, P. Hubert, Promoting Vaginal Distribution of E7 and MCL-1 siRNA-Silencing Nanoparticles for Cervical Cancer Treatment, Mol. Pharm. 14 (2017) 1706–1717. https://doi.org/10.1021/acs.molpharmaceut.6b01154.

[30] A. Lechanteur, T. Furst, B. Evrard, P. Delvenne, P. Hubert, G. Piel, PEGylation of lipoplexes: The right balance between cytotoxicity and siRNA effectiveness, Eur. J.

Pharm. Sci. 93 (2016) 493–503. https://doi.org/10.1016/j.ejps.2016.08.058.

[31] T. Furst, G.R. Dakwar, E. Zagato, A. Lechanteur, K. Remaut, B. Evrard, K. Braeckmans, G. Piel, Freeze-dried mucoadhesive polymeric system containing pegylated lipoplexes: Towards a vaginal sustained released system for siRNA, J. Control. Release. 236 (2016) 68–78. https://doi.org/10.1016/j.jconrel.2016.06.028.

[32] T. Furst, V. Bettonville, E. Farcas, A. Frere, A. Lechanteur, B. Evrard, M. Fillet, G. Piel, A.C. Servais, Capillary electrophoresis method to determine siRNA complexation with cationic liposomes, Electrophoresis. 37 (2016) 2685–2691. https://doi.org/10.1002/elps.201600249.

[33] A. Mechler, S. Praporski, K. Atmuri, M. Boland, F. Separovic, L.L. Martin, Specific and selective peptide-membrane interactions revealed using quartz crystal microbalance, Biophys. J. 93 (2007) 3907–3916. https://doi.org/10.1529/biophysj.107.116525.

[34] T. John, Z.X. Voo, C. Kubeil, B. Abel, B. Graham, L. Spiccia, L.L. Martin, Effects of guanidino modified aminoglycosides on mammalian membranes studied using a quartz crystal microbalance, Medchemcomm. 8 (2017) 1112–1120. https://doi.org/10.1039/c7md00054e.

[35] R. Karim, C. Palazzo, J. Laloy, A.S. Delvigne, S. Vanslambrouck, C. Jerome, E. Lepeltier, F. Orange, J.M. Dogne, B. Evrard, C. Passirani, G. Piel, Development and evaluation of injectable nanosized drug delivery systems for apigenin, Int. J. Pharm. 532 (2017) 757–768. https://doi.org/10.1016/j.ijpharm.2017.04.064.

[36] J. Laloy, V. Minet, L. Alpan, F. Mullier, S. Beken, O. Toussaint, S. Lucas, J.M. Dogné, Impact of Silver Nanoparticles on Haemolysis, Platelet Function and Coagulation,

Nanobiomedicine. 1 (2014) 1–9. https://doi.org/10.5772/59346.

[37] S.Z. Zard, Discovery of the RAFT/MADIX Process: Mechanistic Insights and Polymer Chemistry Implications, Macromolecules. 53 (2020) 8144–8159. https://doi.org/10.1021/acs.macromol.0c01441.

[38] S. Perrier, 50th Anniversary Perspective: RAFT Polymerization - A User Guide, Macromolecules. 50 (2017) 7433–7447. https://doi.org/10.1021/acs.macromol.7b00767.

[39] N. Roka, O. Kokkorogianni, P. Kontoes-Georgoudakis, I. Choinopoulos, M. Pitsikalis, Recent Advances in the Synthesis of Complex Macromolecular Architectures Based on Poly(N-vinyl pyrrolidone) and the RAFT Polymerization Technique, Polymers (Basel). 14 (2022). https://doi.org/10.3390/polym14040701.

[40] B. Tilottama, K. Manojkumar, P.M. Haribabu, K. Vijayakrishna, A short review on RAFT polymerization of less activated monomers, J. Macromol. Sci. Part A Pure Appl. Chem. 59 (2022) 180–201. https://doi.org/10.1080/10601325.2021.2024076.

[41] G. Pound, J.M. McKenzie, R.F.M. Lange, B. Klumperman, Polymer-protein conjugates from ω-aldehyde endfunctional poly(N-vinylpyrrolidone) synthesised via xanthate-mediated living radical polymerisation, Chem. Commun. (2008) 3193–3195. https://doi.org/10.1039/b803952f.

[42] M. Langlais, O. Coutelier, M. Destarac, Thiolactone-Functional Reversible Deactivation Radical Polymerization Agents for Advanced Macromolecular Engineering, Macromolecules. 51 (2018) 4315–4324. https://doi.org/10.1021/acs.macromol.8b00770.

[43] M. Destarac, C. Kalai, A. Wilczewska, L. Petit, E. Van Gramberen, S.Z. Zard, Various strategies for the chemical transformation of xanthate-functional chain termini in MADIX

copolymers, ACS Symp. Ser. 944 (2006) 564–577. https://doi.org/10.1021/bk-2006-0944.ch038.

[44] Y. Xia, J. Tian, X. Chen, Effect of surface properties on liposomal siRNA delivery, Biomaterials. 79 (2016) 56–68. https://doi.org/10.1016/j.biomaterials.2015.11.056.

[45] M.C. Dixon, Quartz crystal microbalance with dissipation monitoring: Enabling real-time characterization of biological materials and their interactions, J. Biomol. Tech. 19 (2008) 151–158.

[46] G. Sauerbrey, Verwendung von Schwingquarzen zur Wägung dünner Schichten und zur Mikrowägung, Zeitschrift Für Phys. 155 (1959) 206–222. https://doi.org/10.1007/BF01337937.

[47] H.R. Jia, Y.X. Zhu, Q.Y. Duan, Z. Chen, F.G. Wu, Nanomaterials meet zebrafish: Toxicity evaluation and drug delivery applications, J. Control. Release. 311–312 (2019) 301–318. https://doi.org/10.1016/j.jconrel.2019.08.022.

[48] K.Y. Lee, G.H. Jang, C.H. Byun, M. Jeun, P.C. Searson, K.H. Lee, Zebrafish models for functional and toxicological screening of nanoscale drug delivery systems: Promoting preclinical applications, Biosci. Rep. 37 (2017) 1–13. https://doi.org/10.1042/BSR20170199.

[49] A. Ledoux, A. St-Gelais, E. Cieckiewicz, O. Jansen, A. Bordignon, B. Illien, N. Di Giovanni, A. Marvilliers, F. Hoareau, H. Pendeville, J. Quetin-Leclercq, M. Frédérich, Antimalarial Activities of Alkyl Cyclohexenone Derivatives Isolated from the Leaves of Poupartia borbonica, J. Nat. Prod. 80 (2017) 1750–1757. https://doi.org/10.1021/acs.jnatprod.6b01019.

[50] S. Sieber, P. Grossen, P. Uhl, P. Detampel, W. Mier, D. Witzigmann, J. Huwyler, Zebrafish as a predictive screening model to assess macrophage clearance of liposomes in vivo, Nanomedicine Nanotechnology, Biol. Med. 17 (2019) 82–93. https://doi.org/10.1016/j.nano.2018.11.017.

[51] S. Ben Djemaa, E. Munnier, I. Chourpa, E. Allard-Vannier, S. David, Versatile electrostatically assembled polymeric siRNA nanovectors: Can they overcome the limits of siRNA tumor delivery?, Int. J. Pharm. 567 (2019). https://doi.org/10.1016/j.ijpharm.2019.06.023.

[52] M. Dominska, D.M. Dykxhoorn, Breaking down the barriers: siRNA delivery and endosome escape, J Cell Sci. 123 (2010) 1183–1189. https://doi.org/10.1242/jcs.066399.

[53] D. Reischl, A. Zimmer, Drug delivery of siRNA therapeutics: potentials and limits of nanosystems, Nanomedicine Nanotechnology, Biol. Med. 5 (2009) 8–20. https://doi.org/10.1016/J.NANO.2008.06.001.

[54] M. Videira, A. Arranja, D. Rafael, R. Gaspar, Preclinical development of siRNA therapeutics: Towards the match between fundamental science and engineered systems, Nanomedicine Nanotechnology, Biol. Med. 10 (2014) 689–702. https://doi.org/10.1016/j.nano.2013.11.018.

[55] M. Kanamala, B.D. Palmer, H. Ghandehari, W.R. Wilson, Z. Wu, PEG-Benzaldehyde-Hydrazone-Lipid Based PEG-Sheddable pH-Sensitive Liposomes: Abilities for Endosomal Escape and Long Circulation, Pharm. Res. 35 (2018) 1–13. https://doi.org/10.1007/S11095-018-2429-Y/TABLES/4.

[56] I. Takeuchi, Y. Kanno, H. Uchiro, K. Makino, Polyborane-encapsulated PEGylated

Liposomes Prepared Using Post-insertion Technique for Boron Neutron Capture Therapy, J. Oleo Sci. 68 (2019) 1261–1270. https://doi.org/10.5650/JOS.ESS19218.

[57] C. Weber, M. Voigt, J. Simon, A.K. Danner, H. Frey, V. Mailänder, M. Helm, S. Morsbach, K. Landfester, Functionalization of Liposomes with Hydrophilic Polymers Results in Macrophage Uptake Independent of the Protein Corona, Biomacromolecules. 20 (2019) 2989–2999. https://doi.org/10.1021/ACS.BIOMAC.9B00539/SUPPL_FILE/BM9B00539_SI_002.XLSX.

[58] Z.A. Bachir, Y.K. Huang, M.Y. He, L. Huang, X.Y. Hou, R.J. Chen, F. Gao, Effects of PEG surface density and chain length on the pharmacokinetics and biodistribution of methotrexate-loaded chitosan nanoparticles, Int. J. Nanomedicine. 13 (2018) 5657–5671. https://doi.org/10.2147/IJN.S167443.

[59] M. Elsabahy, K.L. Wooley, Cytokines as biomarkers of nanoparticle immunotoxicity, Chem. Soc. Rev. 42 (2013) 5552–5576. https://doi.org/10.1039/c3cs60064e.

[60] P. Bigini, M. Gobbi, L. Bonati, A. Clavenna, M. Zucchetti, S. Garattini, G. Pasut, The role and impact of polyethylene glycol on anaphylactic reactions to COVID-19 nano-vaccines, Nat. Nanotechnol. 16 (2021) 1164–1168. https://doi.org/10.1038/s41565-021-01001-3.